Immunology Letters 129 (2010) 39–46

Contents lists available at ScienceDirect

Immunology Letters

journal homepage: www.elsevier.com/locate/

Expression of CD45 isoforms correlates with differential proliferative responses of peripheral CD4$^+$ and CD8$^+$ T cells

Iwao Seki[a,b], Mihoko Suzuki[a], Nobuyuki Miyasaka[a], Hitoshi Kohsaka[a,c,*]

[a] Department of Medicine and Rheumatology, Graduate School, Tokyo Medical and Dental University, Tokyo, Japan
[b] Research and Development Center, Santen Pharmaceutical Co., Ltd., Nara, Japan
[c] Clinical Immunology Laboratory, RIKEN Research Center for Allergy and Immunology, Yokohama, Japan

ARTICLE INFO

Article history:
Received 22 July 2009
Received in revised form 2 December 2009
Accepted 23 December 2009
Available online 20 January 2010

Keywords:
T cells
Protein tyrosine phosphatase
CD45
Cell proliferation
Jak
STAT
IL-2

ABSTRACT

CD4$^+$ T cells express IL-2 receptor complexes to the same level as CD8$^+$ T cells when the two T cell populations were stimulated simultaneously. However, the activation of downstream signaling molecules, such as Jaks, was increased in CD8$^+$ T cells. Although equivalent amounts of CD45, which acts as a Jak phosphatase, was expressed on the two T cell populations, those on the CD8$^+$ T cells have less protein tyrosine phosphatase activity than those on the CD4$^+$ T cells. Furthermore, we find that different CD45 isoforms dominate in the two populations; CD45RO on proliferating CD4$^+$ T cells and CD45RBC on proliferating CD8$^+$ T cells. In addition, NIH3T3 cells expressing the CD45RBC transgene had more phosphorylated Jak1 and grew faster than those with the CD45RO transgene. Thus, the expression of specific CD45 isoforms on T cells correlates with their proliferative response to IL-2, suggesting that controlling cells expressing specific CD45 isoforms could correct excessive or insufficient immune responses.

1. Introduction

CD8$^+$ T cells, unlike CD4$^+$ T cells, are known to undergo extensive clonal expansion in response to viral infection [1–3]. The expanded cells are prone to persist, and thus clonal expansions of CD8$^+$ T cells are frequently found in the peripheral blood from healthy individuals [4,5]. This is more frequent in the elderly than in the young where they can occupy as much as 40% of the total peripheral T cell repertoire [4–6]. This age-related increase in clonal expansion may be responsible for impaired immunocompetence in the elderly. Also, we found that expansion of pathogenic CD8$^+$ T cell clones persist in the peripheral blood of patients with polymyositis, a chronic cytotoxic CD8$^+$ T cell-driven autoimmune disease [7]. The clonal expansions remained even after treatment of the disease and might lead to relapse. The expansions of CD8$^+$ T cells must be partly attributable to the fact that they can be easily activated by promiscuous TCR stimuli [8]. However, the molecular basis for their massive expansion in response to IL-2 in comparison with CD4$^+$ T cells has not yet been addressed. Investigating the specific mechanisms of CD8$^+$ T cell proliferation could help us to develop new therapeutic strategies to reverse immunological senescence and to suppress CD8$^+$ T cell-mediated autoimmunity.

Because T cell expansion subsequent to triggering of antigen receptors is regulated largely by cytokines that stimulate common γ chain cytokine receptors (γc) [9–12], pharmacological inhibition of the γc signaling pathways represents a promising approach for the treatment of autoimmune diseases [13,14]. However, suppression of these cytokines can inhibit proliferation of T cells engaged in both normal and abnormal immune responses, and might induce generalized immune suppression. To minimize the risk of immune suppression, treatment for autoimmune disease should target specific molecules other than γc and/or specific cells associated with the pathogenic responses.

To determine the possibility of treating CD8$^+$ T cell-mediated autoimmune diseases through a disease specific molecular targeting approach, we investigated the γc signaling pathway in CD4$^+$ and CD8$^+$ T cell subsets and aimed to find regulatory molecules which are specific to CD8$^+$ T cell proliferation using an *in vitro* study system. In this study system, CD8$^+$ T cells expand more vigorously and frequently than CD4$^+$ T cells, as was reported in an *in vivo* system [1] and we found that CD45, one of the regulatory molecules of γc signaling pathways [15], was differentially expressed and active in each T cell subset.

CD45 is a transmembrane glycoprotein that has two tandemly duplicated protein tyrosine phosphatase (PTPase) homology

* Corresponding author at: Department of Medicine and Rheumatology, Graduate School, Tokyo Medical and Dental University, 1-5-45 Yushima, Bunkyo-ku, Tokyo 113-8519, Japan. Tel.: +81 3 5803 5204x5209; fax: +81 3 5803 5998.
E-mail address: kohsaka.rheu@tmd.ac.jp (H. Kohsaka).

0165-2478/$ – see front matter © 2010 Elsevier B.V. All rights reserved.
doi:10.1016/j.imlet.2009.12.020

domains in its long cytoplasmic tail [16,17]. It regulates signaling of two types of receptors on T cells; it dephosphorylates the Src family protein tyrosine kinases, Lck and Fyn, to potentiate antigen receptor signaling [18,19] and also functions as a Jak PTPase to attenuate cytokine receptor signaling [15]. A number of mechanisms are hypothesized for the regulation of CD45 PTPase activity: (1) CD45 homo-dimerization, which is modulated by sialylation and O-glycosylation of the extracellular domain [20], (2) CD45-associated protein, which inhibits CD45 homo-dimerization [21], and (3) casein kinase 2, which phosphorylate CD45 [22]. However, the precise mechanisms are still unclear.

CD45 molecules are expressed in several configurations on the cell surface. This is because of alternative splicing of three exons (A, B, and C) that encode its extracellular domains. Although alternative splicing can theoretically recombine the three exons to generate eight different CD45 isoforms, only five isoforms (CD45RO, RB, RAB, RBC, and RABC) are expressed as proteins at significant levels in human or murine lymphocytes [23,24]. Differential function of the distinct CD45 isoforms has been suggested, although the data is inconclusive. Bottomly and her coworkers reported that a $CD4^+$ T cell line expressing the CD45RO isoform preferentially activates the Ras-MAP kinase signaling pathway compared with those expressing the CD45RABC isoform when stimulated with antigen [25]. They also showed that CD45RO was more effective in triggering antigen receptor signaling than the CD45RABC and BC isoforms in T cell lines [26] while a second report disclosed contradictory results [27].

For this study we assumed that CD45 isoform regulation could dictate the differential proliferation of $CD4^+$ and $CD8^+$ T cells, and might be a target for therapeutic intervention in human diseases. We first report that the differential IL-2-induced proliferative response between $CD4^+$ and $CD8^+$ T cells is because of the difference in their IL-2-sensitivity. We also show that the CD45 isoforms on activated $CD8^+$ T cells in the periphery are distinct from those on $CD4^+$ T cells. Because the major CD45 isoform on the $CD8^+$ T cells was not detected on $CD4^+$ T cells, targeting that CD45 isoform could become a new therapeutic strategy for $CD8^+$ T cell-mediated immune abnormalities.

2. Materials and methods

2.1. Mice

C57BL/6J mice were purchased from the Charles River Laboratories Japan Inc. (Kanagawa, Japan). All animal experiments were performed in accordance with the Guidelines for the Care and Use of Laboratory Animals approved by Tokyo Medical and Dental University.

2.2. Cells

Splenic T cells were prepared from 7- to 10-week-old mice using a pan T cell isolation kit (Miltenyi Biotec, Auburn, CA). T cells were stained with anti-CD62L (MEL-14; BD Pharmingen, San Diego, CA) and anti-CD44 mAbs (IM7; BD Pharmingen) to collect naive $CD62L^+CD44^{low}$ T cells using an EPICS ELITE cell sorter (Beckman Coulter, Hialeah, FL). In some experiments, $CD4^+$ and $CD8^+$ T cells were positively selected with anti-CD4 and CD8 conjugated magnetic microbeads (Miltenyi Biotec). Cultures were maintained in RPMI 1640 (Sigma–Aldrich, St. Louis, MO) containing 10% FBS (Hyclone, Logan, UT), 50 μM 2-ME, penicillin G, and streptomycin (Invitrogen, Carlsbad, CA). A murine NIH3T3 fibroblast cell line was purchased from the American Type Culture Collection (Manassas, VA) and maintained in DMEM (Sigma–Aldrich) containing 10% FBS, penicillin G, and streptomycin. Retroviral NIH3T3 transfectants were maintained under the same conditions except for the addition of 4 μg/ml puromycin (Calbiochem, La Jolla, CA).

2.3. Transgene construction and generation of retroviral NIH3T3 transfectants

Full length cDNA of mouse CD45 was isolated by PCR from the pARV-BC and pARV-CD45null plasmid [28], which contained mouse CD45RBC and CD45RO cDNAs, respectively. They were subcloned into the pMXs-IRES-puro retroviral vector (pMXs-IP) [29] using the In Fusion kit (Takara Bio Inc., Shiga, Japan). The recombinant pMXs-IP and control pMXs-IRES-EGFP vectors [29] were transfected into PLAT-E packaging cells [29] using Fugene 6 (Roche Applied Science, Indianapolis, IN). NIH3T3 cells were infected with the recombinant viruses in the presence of 8 μg/ml polybrene(R) (Sigma–Aldrich).

2.4. Proliferation assays

T cells from C57BL/6J mice were stimulated with immobilized anti-CD3ε mAbs (145-2C11, BD Pharmingen) in the presence or absence of 5 μg/ml anti-CD28 mAbs (37.51, BD Pharmingen) for 3 days and then cultured with 100 U/ml recombinant human IL-2 (R&D systems, Minneapolis, MN). Some T cells were treated with a synthetic CD45 inhibitor, dephostatin (Sigma–Aldrich), 30 min before supplementation of IL-2. Proliferation of T cells was assessed by cell counting and flow cytometry. Division of T cells was assessed with CFSE labeling using the CFDA SE cell tracer kit (Invitrogen) and apoptotic cell death of T cells was determined by 7-Amino Actinomycin D (7-AAD) and annexin V staining (Annexin V-FITC/7-AAD kit, Beckman Coulter). NIH3T3 transfectants were plated at 5×10^3 cells per micro-titer well and pulsed with $[^3H]$thymidine for 12 or 24 h to assess their thymidine incorporation.

2.5. Flow cytometry

Anti-CD4, CD25, CD122, and CD132 (H129.19, PC-61, TM-β1, and 4G3, BD Pharmingen), anti-CD8 (KT3, Beckman Coulter), and anti-CD45 (104-2, Southern Biotechnology Associates, Birmingham, AL) mAbs were used for cell staining.

2.6. Immunoblotting and immunoprecipitation

Cells were lysed with ice-cold RIPA lysis buffer (Upstate Biotechnology) with protease inhibitor cocktails (Roche diagnostics, Basel, Switzerland). Whole cell lysates were immunoprecipitated with anti-Jak3 mAbs (B32-32, Sigma–Aldrich) using the Protein G immunoprecipitation kit (Sigma–Aldrich). SDS-PAGE fractionated whole cell lysates or immunoprecipitates were probed with Abs reactive to phosho-Jak1 (pJak1), phospho-STAT5 (pSTAT5), phosho-ERK (pERK), Akt, phospho-Akt (pAkt) (Cell Signaling Technology, Beverly, MA), Jak1, Jak3 (Sigma–Aldrich), ERK, phosphotyrosine, casein kinase 2 (Upstate Biotechnology, Waltham, MA), or CD45-associated protein [30]. CD45 molecules were stained with mAbs reactive to a common epitope shared by all CD45 isoforms (anti-pan-CD45 Abs, Santa Cruz Biotechnology, Santa Cruz, CA), exon A, exon B, or exon C-dependent epitopes of CD45 protein (14.8, 16.A, or DNL-1.9, BD Pharmingen). The bound Abs were visualized with ECL (Amersham Biosciences) using HRP-conjugated anti-rabbit IgG (Amersham Biosciences, Buckinghamshire, UK), or HRP-conjugated anti-mouse IgG (Southern Biotechnology Associates).

2.7. Measurement of CD45 activity

Activity of CD45 protein tyrosine phosphatase was assessed as described elsewhere [31]. Naive ($CD62^+CD44^{low}$) $CD4^+$ and $CD8^+$ T cells cell were stimulated with immobilized anti-CD3ε mAbs for 3 days and then cultured with IL-2 for 5 days. Proteins immunoprecipitated from each T cell lysate with anti-CD45 mAbs (104-2) were incubated with phosphotyrosine peptide (Biomol, Plymouth Meeting, PA). Dephosphorylation reactions were stopped by the addition of Malachite Green reagent (Biomol) and the OD at 650 nm was measured. The amount of total CD45 in the lysates was evaluated by sandwich ELISA using mouse anti-CD45 mAbs (104-2), rat anti-CD45 mAbs (YW62.3, Oxford Biotechnology, UK), and HRP-conjugated anti-rat IgG (Southern Biotechnology Associates). Bound antibodies were quantified with TMB (Zymed Laboratories, South San Francisco, CA) as a substrate.

2.8. Statistical analysis

All values were expressed as means ± SE, and statistically examined with Student's *t*-test using Exsas software (version 7.12; Arm, Osaka, Japan).

3. Results

3.1. $CD8^+$ T cells are more susceptible to in vitro proliferative stimuli than $CD4^+$ T cells

Splenic $CD4^+$ and $CD8^+$ T cells from C57BL/6J mice were stimulated *in vitro* with immobilized anti-CD3ε mAbs, and then with IL-2. In response to this stimulation, $CD8^+$ T cells expanded at a substantially higher rate than $CD4^+$ T cells during the entire culture period (Fig. 1A). In 5 days, the $CD8^+$ T cells that initially had consisted of a minor population compared with $CD4^+$ T cells grew to be the dominant population (Fig. 1B). CFSE labeling of the cells showed that $CD8^+$ T cells divided at a faster rate than $CD4^+$ T cells in response to this stimulation (Fig. 1C) with little difference in the percentage of apoptotic cells (Fig. 1D). Similar proliferative differences were also observed when anti-CD28 mAb was included (Fig. 1E). It has been shown that memory T cells respond more rapidly than naive T cells to antigens [32,33]. Staining of the splenic $CD4^+$ and $CD8^+$ T cells from C57BL/6J mice with CD62L and CD44 mAbs revealed that the $CD8^+$ T cells contained more cells with a $CD62L^+CD44^{high}$ memory phenotype than $CD4^+$ T cells (Fig. 1F). This bias in the naive/memory T cell ratio might be responsible for the proliferative

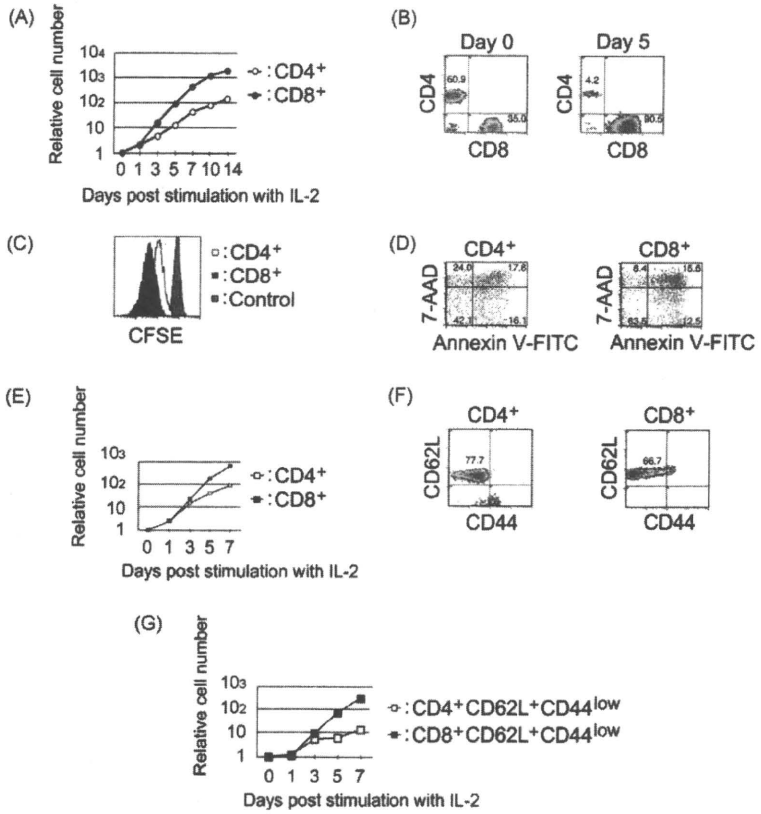

Fig. 1. $CD8^+$ T cells expand more rapidly than $CD4^+$ T cells following *in vitro* stimulation. Splenic T cells from C57BL/6J mice were stimulated with immobilized anti-CD3ε mAbs for 3 days and then cultured with IL-2 for 2 weeks. (A) $CD4^+$ (○) and $CD8^+$ (●) T cell numbers relative to their respective cell numbers at initiation of IL-2 stimulation are shown. Data is representative of three independent experiments. (B) T cells before (day 0: the *left panel*) and 5 days (the *right panel*) after stimulation with IL-2 were stained with anti-CD4 and CD8 mAbs. The percentages of $CD4^+$ and $CD8^+$ T cells in the culture are shown. Data is representative of three independent experiments. (C) Splenic T cells from C57BL/6J mice were stimulated with immobilized anti-CD3ε mAbs for 3 days and then cultured with IL-2 following CFSE labeling. T cells at 3 days post-stimulation with IL-2 were stained with anti-CD4 or CD8 mAbs and the CFSE intensity of $CD4^+$ (□) and $CD8^+$ (■) T cells was analyzed. The CFSE intensity of T cells before the IL-2 stimulation is shown as control staining. Data is representative of two independent experiments. (D) Splenic T cells from C57BL/6J mice were stimulated in the same way, and stained with FITC-conjugated annexin V and 7-AAD instead of CFSE. The percentages of annexin V and/or 7-AAD positive T cells in the culture are shown. Data is representative of two independent experiments. (E) Splenic T cells from C57BL/6J mice were stimulated with immobilized anti-CD3ε mAbs together with soluble anti-CD28 mAbs for 3 days and then cultured with IL-2 for 1 week. $CD4^+$ (□) and $CD8^+$ (■) T cell numbers relative to their respective cell number at initiation of IL-2 stimulation are shown. Representative data of two independent experiments are shown. (F) Splenic T cells from C57BL/6J mice stained with anti-CD62L and CD44 mAbs were analyzed. Flow cytometry data is representative of two independent experiments. (G) Proliferation of naive ($CD62L^+CD44^{low}$) T cells cultured for 2 weeks. Naive T cells from C57BL/6J mice were stimulated with immobilized anti-CD3ε mAbs together with soluble anti-CD28 mAbs for 3 days and then cultured with IL-2. Naive $CD4^+$ (□) and $CD8^+$ (■) T cell numbers relative to their respective cell numbers at initiation of IL-2 stimulation are shown. Data is representative of two independent experiments.

difference between CD4$^+$ and CD8$^+$ T cell preparations. Thus, we purified CD62L$^+$CD44^{low} naive T cell populations to stimulate them with anti-CD3ε mAbs and IL-2. Dominant CD8$^+$ T cell proliferation was observed even among the naive T cells (Fig. 1G).

3.2. IL-2-induces Jak phosphorylation more intensively in CD8$^+$ T cells than in CD4$^+$ T cells

The differential proliferative response of CD4$^+$ and CD8$^+$ T cells has been attributed to the differential upregulation of IL-2 receptor complexes on anti-CD3ε mAb stimulation and/or differential signal transduction through the IL-2 receptor. To test these possibilities, T cells stimulated with anti-CD3ε mAbs for 72 h were examined for their expression of IL-2 receptor α, β, and γ components (CD25, CD122, and CD132). CD25 is equally expressed by the two populations while CD122 and CD132 were increased in CD4$^+$ T cells (Fig. 2A). Thus, the IL-2 receptor expression cannot account for the differential response to IL-2.

Immunoblot analyses of cell lysates from the IL-2 stimulated T cells showed that phosphorylation of Jak1 and Jak3, which are phosphorylated following IL-2 stimulation, was increased in CD8$^+$ T cells (Fig. 2B and C). Reflecting this hyperphosphorylation of Jaks in CD8$^+$ T cells, phosphorylation of STAT5, Akt, and ERK was also increased in CD8$^+$ T cells (Fig. 2D–F). Since expression of the IL-2 receptor complex was not increased in CD8$^+$ T cells, these results showed that CD8$^+$ T cells express IL-2 receptor complexes more susceptible to IL-2 stimulation than CD4$^+$ T cells.

3.3. CD45 protein tyrosine phosphatase activity is significantly higher in CD8$^+$ T cells than in CD4$^+$ T cells

It is known that CD45 PTPase activity potentiates signaling through T cell antigen receptors. At the same time, CD45 attenuates cytokine receptor signaling through Jak, since cytokine receptor signaling depends on Jak dephosphorylation by CD45 [18,19]. Hyperphosphorylation of Jaks and their substrates might be because of lower CD45 PTPase activity in CD8$^+$ T cells. Immunoprecipitated CD45 from CD8$^+$ T cell lysates dephosphorylated tyrosine phosphorylated peptides less efficiently than CD45 from CD4$^+$ T cell lysates (Fig. 3A) while the amount of CD45 in the lysates was equal (Fig. 3B). This demonstrated that the two types of cells had different PTPase activity.

To determine if this difference contributes to the dominant proliferation of CD8$^+$ T cells over CD4$^+$ T cells, dephostatin, a synthetic CD45 PTPase inhibitor, was added to the culture medium in the T cell proliferation assay. Pre-treatment with dephostatin enhanced T cell Jak1 and STAT5 phosphorylation in a concentration-dependent manner (Fig. 3C and D). Dephostatin also promoted proliferation of CD4$^+$ more than that of CD8$^+$ T cells and the ratio of CD8$^+$/4$^+$ T cell number decreased in a concentration-dependent manner (Fig. 3E). We also examined the levels of CD45-associated protein and casein kinase 2 in each T cell subset, both reported to regulate CD45 PTPase activity [21,22], and found no differences between the CD4$^+$ and CD8$^+$ T cell populations (Fig. 3F and G). These results showed that pharmacological attenuation of CD45 PTPase activity, resulting in enhanced activation of IL-2 receptor signaling, might bring CD4$^+$ T cells close to CD8$^+$ T cells in terms of their proliferative response.

3.4. CD4$^+$ and CD8$^+$ T cells express distinct CD45 isoforms

As was stated earlier, one of the factors dictating CD45 PTPase activity is their isoform. To identify CD45 isoforms expressed by the activated CD4$^+$ and CD8$^+$ T cells, they were fractionated and examined with immunoblot analyses using Ab that recognize

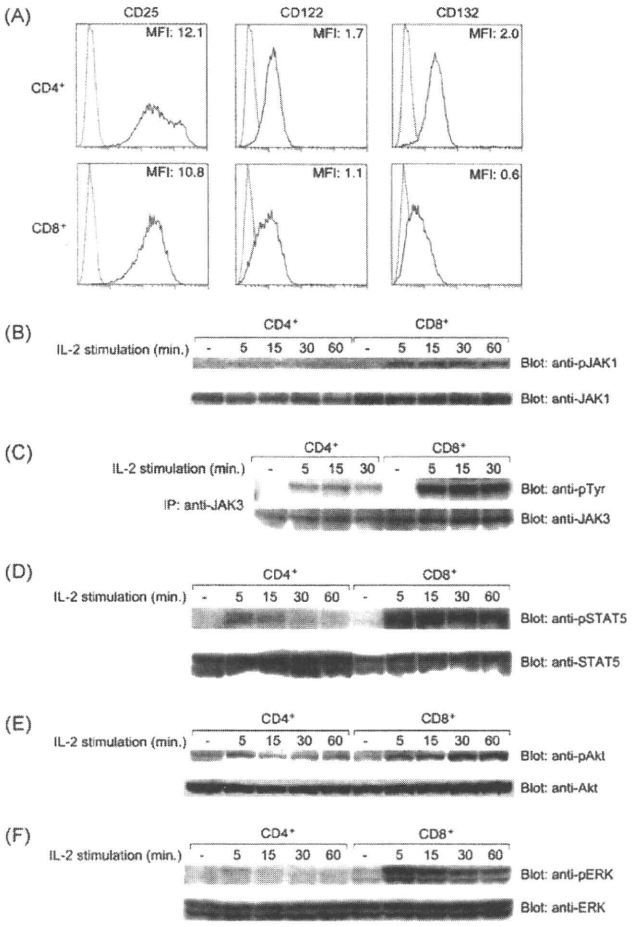

Fig. 2. IL-2 receptor complex expression is reduced but IL-2-triggered signaling is transduced more efficiently in CD8$^+$ T cells than in CD4$^+$ T cells. Splenic CD4$^+$ and CD8$^+$ T cells from C57BL/6J mice were stimulated with immobilized anti-CD3ε mAbs for 3 days and then cultured with IL-2 for 5 days. (A) Surface CD25, CD122, and CD132 molecules on CD4$^+$ and CD8$^+$ T cells were stained with specific mAbs (solid lines) or isotype control Abs (dotted lines), and analyzed by flow cytometry. The mean fluorescence intensity (MFI) of each sample is shown. (B–F) CD4$^+$ and CD8$^+$ T cells were stimulated and cultured as in (A). They were then stimulated with IL-2 and lysed at the indicated time points after initiation of IL-2 stimulation. pJak1 (B, the *upper panel*) and Jak1 (B, the *lower panel*) in the same lysates were immunodetected with specific Abs. Jak3 proteins were immunoprecipitated from the cell lysates with specific Ab and immunoblotted with anti-phosphotyrosine mAbs (C, the *upper panel*) and with Abs against Jak3 (C, the *lower panel*). pJak1, pSTAT5, pAkt, and pERK (D–F, the *upper panels*, respectively) and Jak1, STAT5, Akt, and ERK (D–F, the *lower panels*, respectively) were detected as in B. Immunoblots and flow cytometric analyses are representative of three independent experiments.

all CD45 isoforms. This method revealed that CD4$^+$ and CD8$^+$ T cells expressed CD45 molecules with distinct molecular weights: 180 kDa by CD4$^+$ T cells and 210 kDa by CD8$^+$ T cells (Fig. 4A). CD4$^+$ T cells expressed another CD45 molecule to a lesser extent with a molecular weight of 190 kDa. Considering the contribution of each exon product in the total molecular weight of CD45, the major CD45 isoform expressed by CD4$^+$ T cells is CD45RO, without any alternatively spliced exons, and the minor molecule has an additional exon. CD8$^+$ T cells should express CD45 molecules with two additional exons. On analysis using exon product-specific mAbs, CD45 on proliferating CD4$^+$ T cells contained products of exon B while those on proliferating CD8$^+$ T cells contained products of exons B and C (Fig. 4B). Thus, proliferating CD4$^+$ T cells express CD45RO and CD45RB while proliferating CD8$^+$ T cells express CD45RBC.

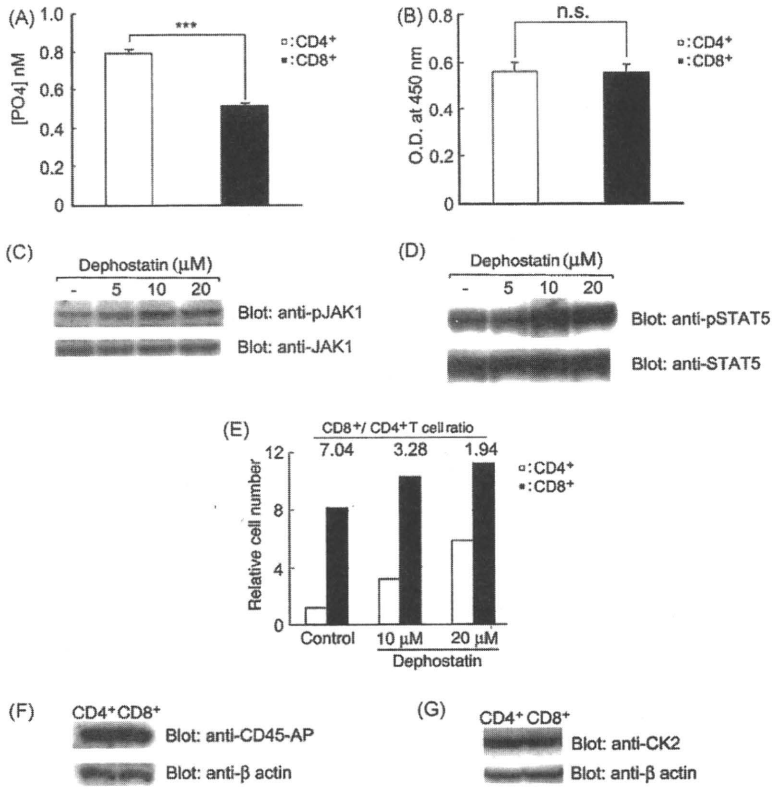

Fig. 3. CD8+ T cells express CD45 with lower tyrosine phosphatase activity than CD4+ T cells. Naive ($CD62^+CD44^{low}$) CD4+ and CD8+ T cells were stimulated with immobilized anti-CD3ε mAbs for 3 days and then cultured with IL-2 for 5 days. (A) The same number of CD4+ (open column) and CD8+ (solid column) T cells were lysed and the CD45 PTPase activity derived from the two populations was quantified with phosphotyrosine peptides as CD45 PTPase substrates. The columns and bars represent the mean and SE of three samples. Data is representative of two independent experiments. ***$P < 0.001$. (B) The amount of total CD45 protein in the lysates from (A) was determined. Data is representative of two independent experiments. (C and D) Splenic T cells from C57BL/6J mice were stimulated and cultured as in Fig. 2A. They were then treated with dephostatin at the indicated concentration followed by supplementation of IL-2. Cells were lysed 5 min after IL-2 stimulation. pJak1 (C, the *upper panel*), Jak1 (C, the *lower panel*), pSTAT5 (D, the *upper panels*) and STAT5 (D, the *lower panels*) in the same lysates were immunodetected with specific Abs. Immunoblot analyses are representative of two independent experiments. (E) Splenic T cells from C57BL/6J mice were activated with immobilized anti-CD3ε mAbs for 3 days and then cultured with IL-2 for 4 days with or without dephostatin. CD4+ (open column) and CD8+ T cell (solid column) numbers are relative to the number of CD4+ T cells without dephostatin treatment in the culture and CD8+/CD4+ T cell ratios are shown. The data is representative of two independent experiments. (F and G) Splenic T cells from C57BL/6J mice were stimulated and cultured as in Fig. 2A. CD4+ and CD8+ T cells were positively selected with anti-CD4 and CD8 conjugated magnetic microbeads for preparing cell lysates. CD45-associated protein (CD45-AP; F, the *upper panel*), casein kinase 2 (CK2; G, the *upper panel*), and β actin (F and G, the *lower panel*) were detected with specific Abs. The data are representative of two independent experiments.

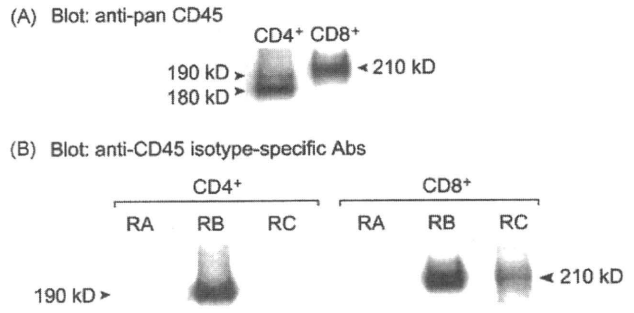

Fig. 4. Activated CD4+ and CD8+ T cells express distinct CD45 isoforms. (A) Naive $CD62L^+CD44^{low}CD4^+$ and CD8+ T cells were stimulated with immobilized anti-CD3ε mAbs for 3 days and then cultured with IL-2 for 5 days. CD45 molecules in SDS-fractionated cell lysates were detected with mAbs against pan-CD45. Molecular weights predicted by molecular mass markers (not shown) are indicated on the sides. (B) The same lysates were blotted for CD45RA, CD45RB, and CD45RC. Molecular weights predicted by molecular mass markers (not shown) are indicated on the sides. The data is representative of two independent experiments.

3.5. CD45 isoforms preferentially expressed by CD4+ and CD8+ T cells contribute to differential cell proliferation

To demonstrate that the dominance of different CD45 isoforms on activated CD4+ or CD8+ T cell populations leads to different Jak PTPase activity and cellular proliferation, the CD45RO and CD45RBC genes were introduced to cells that do not express intrinsic CD45. We therefore retrovirally transfected NIH3T3 fibroblastoid cells with CD45RO or CD45RBC. We used this method because (1) T cells do not develop normally in CD45 null mice [34,35], (2) it is hard to introduce genes into normal T cells or the CD45 negative BW5147($T200^-$) T cell line, (3) a large amount of CD45 molecules are express on primary T cells, making it unreasonable to asses the effects of the CD45 transgenes, (4) NIH3T3 cells do not express CD45 (data not shown), and (5) their Jak1 molecules were phosphorylated constitutively in FBS-supplemented conventional culture medium (Fig. 5A). Although flow cytometric analysis with CD45 Ab showed that CD45RO and CD45RBC-transduced NIH3T3 cells expressed CD45 molecules at comparable levels (Fig. 5B), phosphorylation of Jak1 was especially reduced in the CD45RO-transduced cells compared with control retrovirus-infected cells (Fig. 5A). In concordance with the differential phosphorylation levels of Jak1,

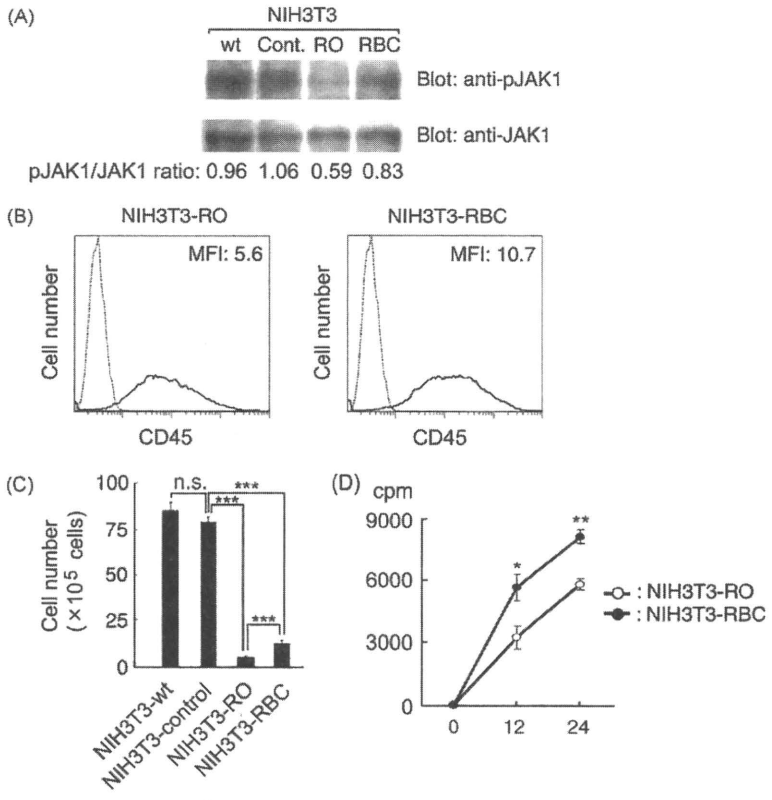

Fig. 5. CD45 has isoform-specific Jak phosphatase activity and inhibits NIH3T3 cell proliferation in a PTPase activity dependent manner. (A) pJak1 (the *upper panel*) and Jak1 (the *lower panel*) in cell lysates from CD45RO and CD45RBC-transduced cells (RO and RBC, respectively), control retrovirus-infected cells (cont.) and unmanipulated NIH3T3 cells (wt) were detected with specific Abs. The levels of pJak1 and Jak1 were quantified using NIH image (version 1.61) and the pJak1/Jak1 ratio was calculated. The data is representative of two independent experiments. (B) CD45 on the transfectants was stained with anti-CD45 mAbs (solid lines) or isotype control Abs (dotted lines), and analyzed by flow cytometry. The mean fluorescence intensity (MFI) of each sample is shown. The data are representative of two independent experiments. (C) Proliferation of unmanipulated NIH3T3 cells (NIH3T3-wt), control retrovirus-infected cells (NIH3T3-control), CD45RO and CD45RBC-transduced cells (NIH3T3-RO and NIH3T3-RBC, respectively) was assessed by cell counting. NIH3T3-wt, NIH3T3-control, NIH3T3-RO, and NIH3T3-RBC cells were plated at 5×10^5 cells per T-25 flask and cultured with 10% FBS containing DMEM for 5 days. The total cell numbers of each cell line at day 5 (5 days after culture) are shown. The columns and bars represent the mean and SE of six samples. Data is representative of two independent experiments. ***$P < 0.001$. (D) Proliferation of CD45RO and CD45RBC-transduced cells (NIH3T3-RO and NIH3T3-RBC, respectively) was assessed by a [^{3}H]thymidine incorporation assay. Assays were performed in triplicate and the data is shown as the mean and SE of three samples. Data is representative of two independent experiments. *$P < 0.05$, **$P < 0.01$ (NIH3T3-RO vs NIH3T3-RBC).

NIH3T3 transfectants expressing CD45RO grew significantly slower than those expressing CD45RBC (Fig. 5C and D). These results show that the difference in CD45 isotype can dictate cellular proliferation through Jak dephosphorylation.

4. Discussion

CD8$^+$ T cells expanded more rapidly than CD4$^+$ T cells in response to IL-2 following anti-CD3ε mAb stimulation *in vitro*. During proliferation, Jak1, Jak3, and other molecules downstream of the IL-2 receptor were more activated in CD8$^+$ T cells than in CD4$^+$ T cells. Activated CD4$^+$ and CD8$^+$ T cells expressed distinct CD45 isoforms that differentially phosphorylated Jaks, leading to differential proliferative responses. Susceptibility of CD4$^+$ and CD8$^+$ T cells to proliferative stimuli appears to be at least partly regulated by CD45 isoform expression.

In contrast to CD4$^+$ T cells, CD8$^+$ T cells undergo extensive expansion following host infection with *Listeria* [1]. There are also many reports of the clonal expansion of CD8$^+$ T cells, not of CD4$^+$ T cells, in normal elderly humans [4,5]. To discern what controls the intrinsic difference in the proliferative responses of CD4$^+$ and CD8$^+$ T cells, we employed an *in vitro* system that mimicked the CD8$^+$ T cell-dominating *in vivo* T cell proliferation. Although it is yet to be determined to what extent the CD45 isoforms regulate IL-2 responses *in vivo*, this study provides insight into the dominant proliferative response of CD8$^+$ T cells.

It has been known that proliferation of CD8$^+$ T cells is preferentially driven by IL-7 and IL-15 [10,11]. However, these cytokines were not detected in the culture supernatants (data not shown). CIS, SOCS1, and SOCS3, negative regulators of cytokine signaling in CD4$^+$ and CD8$^+$ T cells [36–38], were equally expressed by both types of T cells expanded with anti-CD3ε mAbs and IL-2 (data not shown). Thus, the dominant proliferative response of CD8$^+$ T cells appears to be attributable solely to the lower Jak PTPase activity of their CD45.

CD45 molecules on human CD4$^+$ T cells have been used as a marker of naive and memory T cells since CD45 isoform expression shifts from CD45RA to CD45RO on stimulation with specific antigens *in vivo* [32]. Although several methods were employed in this study, immunoblot analysis with a panel of CD45 isotype-specific antibodies was the only tool to comprehensively examine cells for their entire CD45 isoform repertoire. This technique was able to detect CD45 isoforms expressed on T cells, although not enough protein could be extracted from cells before activation. We tried PCR to amplify CD45 cDNA derived from CD4$^+$ and CD8$^+$ T cells T cells using primers specific to the exons flanking the alternatively spliced exons. However, possibly because of mispriming of the primers, the amplified products failed to

discriminate any differences in the cDNA sequences (data not shown).

It has been shown that CD45 PTPase activity depends on its isoform [20]. Indeed, Bottomly et al. reported that the CD45RO isoform has higher PTPase activity than the CD45RABC and BC isoforms in T cells [26]. On the other hand, Xu and Weiss proposed that CD45 PTPase activity is regulated by homo-dimerization of CD45 molecules [20]. According to this, CD45RO, which is the least modified isoform, should have lower PTPase activity than CD45RBC. However, the dimer hypothesis is controversial and they did not measure CD45 PTPase activity generally or on Jak kinases. Thus, several factors may account for regulation of CD45 PTPase activity in some experimental settings. One of these molecules is CD45-associated protein [21], which was reported to up-regulate the CD45 PTPase activity. However, no difference in the protein level of CD45-associated protein was observed between $CD4^+$ and $CD8^+$ T cells (data not shown). Other studies suggested that the CD45 PTPase activity is augmented by phosphorylation of specific serine residues by casein kinase 2 [22]. We examined the activated $CD4^+$ and $CD8^+$ T cells for the protein level of casein kinase 2, and failed to see any difference.

We demonstrated here that CD45 on the $CD8^+$ T cells has less protein tyrosine PTPase activity than CD45 expressed on $CD4^+$ T cells, and also different CD45 isoforms dominate in the two populations. In addition, pharmacological inhibition of CD45 activity drove the proliferation of $CD4^+$ T cells close to that of $CD8^+$ T cells. While it was shown that dephostatin did not inhibit serine/threonine phosphatases and protein kinases [39], no inhibitory activity of dephostatin on PTPases other than CD45 has been reported. The involvement of other PTPases in IL-2R signaling of T cells has not been reported. Furthermore, we observed that SHP-1, which can dephosphorylate STAT [40], was equally expressed by $CD4^+$ and $CD8^+$ T cells (data not shown). These facts led us to believe that the events observed in Fig. 3E were because of the inhibitory effect of dephostatin on CD45 activity. However, since the possibility that dephostatin also suppresses other PTPases cannot be ruled out, the use of this pharmacological inhibitor alone is not enough to conclude that differential CD45 PTPase activity is responsible for the proliferative responses of $CD4^+$ and $CD8^+$ T cells. Therefore, we further tested this hypothesis using gene transfer techniques.

Because of the reasons described in Section 3, we introduced the CD45RO and CD45RBC genes into NIH3T3 cells and demonstrated the effects of CD45RO and CD45RBC on Jak1 phosphorylation and proliferation. Although we tried to detect PTPase activity of the NIH3T3 transfectants directly, it was not feasible because the transfectants did not grow rapidly enough to be examined by the dephosphorylation assay. We also tried to check the effects of FBS starvation on JAK1 phosphorylation in NIH3T3 cell to mimic the cytokine-inducible Jak1 activation. However, we could not see a down modulation in Jak1 phosphorylation without introducing cell death. Therefore, we could not clearly show the effects of the CD45 transgenes on cytokine-induced Jak1 phosphorylation and proliferation of the transfectants. However, these data strongly support our hypothesis that specific CD45 isoforms expressed on T cells correlates with their proliferative response to IL-2.

Since the Jak-STAT pathway plays a primary role in lymphocyte proliferation triggered by cytokine receptor signaling [41], pharmacological inhibition of Jaks, STATs, and other related molecules, including cytokines, should be effective in the treatment of autoimmune diseases [42]. In fact, some chemical compounds have been synthesized for this purpose [42,43]. However, these compounds can suppress both normal and abnormal immune responses and thus may induce excessive immune suppression. In contrast, since CD45 positively regulates antigen receptor signaling [17,18], modulating CD45 to up-regulate its PTPase activity should not suppress the initial T cell activation triggered by antigens but instead inhibit inappropriate expansion. Thus, it may offer a new tool to correct abnormal T cell homeostasis in autoimmune diseases.

Acknowledgments

We thank Drs. Toshio Kitamura and Kim Bottomly for providing retroviruses and advice; Dr. Akiko Takeda for providing anti-CD45-associated protein Ab; Drs. Takahiko Sugihara, Yoshinori Nonomura, Chiyoko Sekine, and Hiroyuki Hagiyama for helpful discussions and suggestions. This work was supported by grants-in-aid from the Japanese Ministry of Health, Labor and Welfare, and from the Ministry of Education, Culture, Sports, Science and Technology, Japan.

References

[1] Foulds KE, Zenewicz LA, Shedlock DJ, Jiang J, Troy AE, Shen H. Cutting edge: CD4 and CD8 T cells are intrinsically different in their proliferative responses. J Immunol 2002;168:1528–32.
[2] Murali-Krishna K, Miller JD, Slansky J, Ahmed R. Counting antigen-specific CD8 T cells: a re-evaluation of bystander activation during viral infection. Immunity 1998;8:177–87.
[3] Callan MF, Tan L, Annels N, Ogg GS, Wilson JD, O'Callaghan CA, et al. Direct visualization of antigen-specific $CD8^+$ T cells during the primary immune response to Epstein–Barr virus in vivo. J Exp Med 1998;187:1395–402.
[4] Fitzgerald JE, Ricalton NS, Meyer AC, West SG, Kaplan H, Behrendt C, et al. Analysis of clonal $CD8^+$ T cell expansions in normal individuals and patients with rheumatoid arthritis. J Immunol 1995;154:3538–47.
[5] Posnett DN, Sinha R, Kabak S, Russo C. Clonal populations of T cells in normal elderly humans: the T cell equivalent to "Benign monoclonal gammapathy". J Exp Med 1994;179:609–18.
[6] Schindowski K, Frohlich L, Maurer K, Muller WE, Eckert A. Age-related impairment of human T lymphocytes' activation: specific differences between $CD4^+$ and $CD8^+$ subsets. Mech Ageing Dev 2002;123:375–90.
[7] Nishio J, Suzuki M, Miyasaka N, Kohsaka H. Clonal biases of peripheral CD8 T cell repertoire directly reflects local inflammation in polymyositis. J Immunol 2001;167:4051–8.
[8] Tanchot C, Lemonnier FA, Perarnau B, Freitas AA, Rocha B. Differential requirements for survival and proliferation of CD8 naive or memory T cells. Science 1997;276:2057–62.
[9] Schluns KS, Lefrancois L. Cytokine control of memory T-cell development and survival. Nat Rev Immunol 2003;3:269–79.
[10] Surh CD, Sprent J. Regulation of mature T cell homeostasis. Semin Immunol 2005;17:183–91.
[11] Tan JT, Ernst B, Kieper WC, Leroy E, Sprent J, Surh CD. Interleukin (IL)-15 and IL-7 jointly regulate homeostatic proliferation of memory phenotype $CD8^+$ cells but are not required for memory phenotype $CD4^+$ cells. J Exp Med 2002;195:1523–32.
[12] Kovanen PE, Leonard WJ. Cytokines and immunodeficiency diseases: critical roles of the gamma(c)-dependent cytokines interleukins 2, 4, 7, 9, 15, and 21, and their signaling pathways. Immunol Rev 2004;202:67–83.
[13] Papageorgiou AC, Wikman LE. Is JAK3 a new drug target for immunomodulation-based therapies? Trends Pharmacol Sci 2004;25:558–62.
[14] Ferrari-Lacraz S, Zanelli E, Neuberg M, Donskoy E, Kim YS, Zheng XX, et al. Targeting IL-15 receptor-bearing cells with an antagonist mutant IL-15/Fc protein prevents disease development and progression in murine collagen-induced arthritis. J Immunol 2004;173:5818–26.
[15] Penninger JM, Irie-Sasaki J, Sasaki T, Oliveria-dos-Santos AJ. CD45: new jobs for an old acquaintance. Nat Immunol 2001;2:389–96.
[16] Hermiston ML, Xu Z, Weiss A. CD45: a critical regulator of signaling thresholds in immune cells. Annu Rev Immunol 2003;21:107–37.
[17] Holms N. CD45: all is not yet crystal clear. Immunology 2005;117:145–55.
[18] Koretzky GA, Picus J, Thomas ML, Weiss A. Tyrosine phosphatase CD45 is essential for coupling T cell antigen receptor to the phosphatidylinositol pathway. Nature 1990;346:66–8.
[19] Pingel JT, Thomas ML. Evidence that the leukocyte-common antigen is required for antigen-induced T lymphocyte proliferation. Cell 1989;58:1055–65.
[20] Xu Z, Weiss A. Negative regulation of CD45 by differential homodimerization of the alternatively spliced isoforms. Nat Immunol 2002;3:764–71.
[21] Takeda A, Matsuda A, Paul RM, Yaseen NR. CD45-associated protein inhibits CD45 dimerization and up-regulates its protein tyrosine phosphatase activity. Blood 2004;103:3440–7.
[22] Greer SF, Wang Y, Raman C, Justement LB. CD45 function is regulated by an acidic 19-amino acid insert in domain II that serves as binding and phosphoacceptor site for casein kinase 2. J Immunol 2001;166:7208–18.
[23] Rogers PR, Pilapil S, Hayakawa K, Roman PL, Parker DC. CD45 alternative exon expression in murine and human CD4+ T cell subsets. J Immunol 1992;148:4054–65.
[24] Fukuhara K, Okumura M, Shiono H, Inoue M, Kadota Y, Miyoshi S, et al. A study on CD45 isoform expression during T-cell development and selection events in the human thymus. Hum Immunol 2002;63:394–404.

[25] Czyzyk J, Leitenberg D, Taylor T, Bottomly K. Combinatorial effect of T-cell receptor ligation and CD45 isoform expression on the signaling contribution of the small GTPases Ras and Rap1. Mol Cell Biol 2000;20:8740–7.
[26] Novak TJ, Farber D, Leitenberg D, Hong SC, Johnson P, Bottomly K. Isoforms of the transmembrane tyrosine phosphatase CD45 differentially affect T cell recognition. Immunity 1994;1:109–19.
[27] Chui D, Ong CJ, Johnson P, Teh HS, Marth JD. Specific CD45 isoforms differentially regulate T cell receptor signaling. EMBO J 1994;13:798–807.
[28] Johnson P, Greenbaum L, Bottomly K, Trowbridge IS. Identification of the alternatively spliced exons of murine CD45 (T200) required for reactivity with B220 and other T200-restricted antibodies. J Exp Med 1989;169:1179–84.
[29] Kitamura T, Koshino Y, Shibata F, Oki T, Nakajima H, Nosaka T, et al. Retrovirus-mediated gene transfer and expression cloning: powerful tools in functional genomics. Exp Hematol 2003;31:1007–14.
[30] Kitamura K, Maiti A, Ng DH, Johnson P, Maizel AL, Takeda A. Characterization of the interaction between CD45 and CD45-AP. J Biol Chem 1995;270:21151–7.
[31] Rider DA, Young SP. Measuring the specific activity of the CD45 protein tyrosine phosphatase. J Immunol 2003;277:127–34.
[32] Dutton RW, Bradley LM, Swain SL. T cell memory. Annu Rev Immunol 1998;16:201–23.
[33] Gegnat J, Sallusto F, Lanzavecchia A. Cytokine-driven proliferation and differentiation of human naive, central memory, and effector memory CD4+ T cells. J Exp Med 2001;194:1711–9.
[34] Kishihara K, Penninger J, Wallace VA, Kundig TM, Kwai K, Wakeham A, et al. Normal B lymphocyte development but T cell maturation in CD45-exon6 protein tyrosine phosphatase-deficient mice. Cell 1993;74:143–56.
[35] Byth KF, Conroy LA, Howlett S, Smith AH, May J, Alexander DR, et al. CD45-null transgenic mice reveal a positive regulatory role for CD45 in early thymocyte development, in the selection of CD4+CD8+ thymocytes, and in B cell maturation. J Exp Med 1996;183:1707–18.
[36] Ilangumaran S, Rottapel R. Regulation of cytokine receptor signaling by SOCS1. Immunol Rev 2003;192:196–211.
[37] Yasukawa H, Sasaki A, Yoshimura A. Negative regulation of cytokine signaling pathways. Annu Rev Immunol 2000;18:143–64.
[38] Aman JM, Migone T, Sasaki A, Ascherman DP, Zhu M, Soldani E, et al. CIS associates with the interleukin-2 receptor β chain and inhibits interleukin-2-dependent signaling. J Biol Chem 1999;274:30266–72.
[39] Imoto M, Tanaka S, Deguchi A, Hayakawa A, Umezawa K. In situ inhibition of protein-tyrosine phosphatase by dephostatin. Cell Pharmacol 1995;2:199–203.
[40] Haque SJ, Harbor P, Tabrizi M, Yi T, Williams BRG. Protein-tyrosine phosphatase Shp-1 is a negative regulator of IL-4- and IL-13-dependent signal transduction. J Biol Chem 1998;273:33893–6.
[41] Lord JD, McIntosh BC, Greenberg PD, Nelson BH. The IL-2 receptor promotes lymphocyte proliferation and induction of the c-myc, bcl-2, and bcl-x genes through the trans-activation domain of stat5. J Immunol 2000;164:2533–41.
[42] O'Shea JJ, Park H, Pesu M, Borie D, Changelian P. New strategies for immunosuppression: interfering with cytokines by targeting the Jak/Stat pathway. Curr Opin Rheumatol 2005;17:305–11.
[43] Borie DC, Si MS, Morris RE, Reitz BA, Changelian PS. JAK3 inhibition as a new concept for immune suppression. Curr Opin Invest Drugs 2003;4:1297–303.

ARTHRITIS & RHEUMATISM
Vol. 62, No. 2, February 2010, pp 574–579
DOI 10.1002/art.27190

The Association of a Nonsynonymous Single-Nucleotide Polymorphism in *TNFAIP3* With Systemic Lupus Erythematosus and Rheumatoid Arthritis in the Japanese Population

Kenichi Shimane,[1] Yuta Kochi,[2] Tetsuya Horita,[3] Katsunori Ikari,[4] Hirofumi Amano,[5] Michito Hirakata,[6] Akiko Okamoto,[7] Ryo Yamada,[8] Keiko Myouzen,[2] Akari Suzuki,[2] Michiaki Kubo,[2] Tatsuya Atsumi,[3] Takao Koike,[3] Yoshinari Takasaki,[5] Shigeki Momohara,[4] Hisashi Yamanaka,[4] Yusuke Nakamura,[8] and Kazuhiko Yamamoto[1]

Objective. **Genome-wide association (GWA) studies in systemic lupus erythematosus (SLE) and rheumatoid arthritis (RA) in Caucasian populations have independently identified risk variants in and near the tumor necrosis factor α (TNFα)–induced protein 3 gene (*TNFAIP3*), which is crucial for the regulation of TNF-mediated signaling and Toll-like receptor signaling. The aim of this study was to assess the role of *TNFAIP3* in the development of SLE and RA in Japanese subjects.**

Methods. **We selected 2 single-nucleotide polymorphisms (SNPs) from previous GWA studies. Rs2230926 is a nonsynonymous SNP in *TNFAIP3* and is associated with SLE, while rs10499194 is an intergenic SNP associated with RA. We then performed 2 independent sets of SLE case–control comparisons (717 patients and 1,362 control subjects) and 3 sets of RA case–control comparisons (3,446 patients and 2,344 control subjects) using Japanese subjects. We genotyped SNPs using TaqMan assays.**

Results. **We observed a significant association between rs2230926 and an increased risk of SLE and RA in the Japanese population (for SLE, odds ratio [OR] 1.92, 95% confidence interval [95% CI] 1.53–2.41, $P = 1.9 \times 10^{-8}$; for RA, OR 1.35, 95% CI 1.18–1.56, $P = 2.6 \times 10^{-5}$). The intergenic SNP rs10499194 was also associated with SLE and RA, while the risk allele for RA in Caucasians was protective against the diseases in our population.**

Drs. Shimane, Kochi, Yamada, Myouzen, Suzuki, Kubo, Nakamura, and Yamamoto's work was supported by a grant from the Center for Genomic Medicine (CGM), Institute of Physical and Chemical Research (RIKEN). Drs. Horita, Amano, Hirakata, Okamoto, Yamada, Atsumi, Koike, and Takasaki's work was supported by a grant from the Japanese Ministry of Health, Labor, and Welfare. Drs. Ikari, Momohara, and Yamanaka's work was supported by a Japan Orthopaedics and Traumatology Foundation grant, a Takeda Science Foundation grant, and a Japanese Ministry of Education, Culture, Sports, Science, and Technology grant-in-aid for scientific research. The Institute of Rheumatology Rheumatoid Arthritis cohort was supported by 36 pharmaceutical companies.

[1]Kenichi Shimane, MD, PhD, Kazuhiko Yamamoto, MD, PhD: Graduate School of Medicine, University of Tokyo, Tokyo, Japan, and CGM, RIKEN, Yokohama, Japan; [2]Yuta Kochi, MD, PhD, Keiko Myouzen, MSc, Akari Suzuki, PhD, Michiaki Kubo, MD, PhD: CGM, RIKEN, Yokohama, Japan; [3]Tetsuya Horita, MD, PhD, Tatsuya Atsumi, MD, PhD, Takao Koike, MD, PhD: Hokkaido University Graduate School of Medicine, Sapporo, Japan; [4]Katsunori Ikari, MD, PhD, Shigeki Momohara, MD, PhD, Hisashi Yamanaka, MD, PhD: Tokyo Women's Medical University, Tokyo, Japan; [5]Hirofumi Amano, MD, PhD, Yoshinari Takasaki, MD, PhD: School of Medicine, Juntendo University, Tokyo, Japan; [6]Michito Hirakata, MD, PhD: Keio University School of Medicine, Tokyo, Japan; [7]Akiko Okamoto, MD, PhD: Graduate School of Medicine, University of Tokyo, Tokyo, Japan; [8]Ryo Yamada, MD, PhD, Yusuke Nakamura, MD, PhD: Institute of Medical Science, University of Tokyo, Tokyo, Japan.

Dr. Ikari has received speaking fees from Abbott Japan and Mitsubishi Tanabe Pharma (less than $10,000 each). Dr. Momohara has received speaking fees from Astellas Pharma, Chugai Pharmaceutical, Dainippon Sumitomo Pharma, Kaken Pharmaceutical, Mitsubishi Tanabe Pharma, Sanofi-Aventis, Santen Pharmaceutical, Takeda Pharmaceutical, and Wyeth (less than $10,000 each). Dr. Yamanaka has received speaking fees from Abbott Japan, Chugai Pharmaceutical, Eisai, Mitsubishi Tanabe Pharma, Hoffman-LaRoche, Takeda Pharmaceutical, and Wyeth (less than $10,000 each). Dr. Yamamoto has received consulting fees, speaking fees, or honoraria from Astellas Pharma and Chugai Pharmaceutical (less than $10,000 each) and owns stock or stock options in ImmunoFuture.

Address correspondence and reprint requests to Yuta Kochi, MD, PhD, Laboratory for Autoimmune Diseases, CGM, RIKEN, 7-3-1 Hongo, Bunkyo-Ku, Tokyo 113-0033, Japan. E-mail: ykochi@src.riken.jp.

Submitted for publication May 6, 2009; accepted in revised form October 2, 2009.

Conclusion. **We demonstrated a significant association between the nonsynonymous variant in *TNFAIP3* and the risk for SLE and RA in the Japanese population. *TNFAIP3*, similar to *STAT4* and *IRF5*, may be a common genetic risk factor for SLE and RA that is shared between the Caucasian and Japanese populations.**

Systemic lupus erythematosus (SLE) and rheumatoid arthritis (RA) represent multigenic diseases and are considered to be caused by interactions between susceptibility genes and environmental factors that result in an abnormal immune response. In fact, familial and linkage studies have provided strong evidence for the role of multiple genetic factors in the development of SLE and RA (1). In addition, association-based approaches in candidate loci using single-nucleotide polymorphisms (SNPs) have also identified several genes that contribute to these diseases. More recently, genome-wide association (GWA) studies in SLE and RA have revealed many susceptibility genes and pathways that contribute to disease development (2).

Familial and linkage studies have also shown familial aggregation of RA, SLE, and other immune-mediated diseases (1). In fact, several gene polymorphisms, including *PTPN22*, *STAT4*, and *IRF5* variants, have been shown to predispose to SLE and RA. Recent GWA studies in Caucasian populations have also identified the tumor necrosis factor α (TNFα)–induced protein 3 gene (*TNFAIP3*) as another common genetic risk factor for SLE and RA (3–6). *TNFAIP3*, also known as the A20 protein, is a negative regulator of the NF-κB signaling pathway that is essential in the pathogenesis of both SLE and RA (7). The association of *TNFAIP3* with diseases has been independently reported in SLE and RA, and it is of great interest that the peaks in association in the GWA studies are different between SLE and RA. In Caucasian populations, the significantly associated SNP markers for SLE, including the nonsynonymous SNP termed rs2230926, are located in the *TNFAIP3* region, while those for RA are located in the intergenic region between *TNFAIP3* and the oligodendrocyte transcription factor 3 gene (*OLIG3*). In addition to the difference in the diseases themselves, the association between *TNFAIP3* polymorphisms and these diseases in the Asian populations remains unclear (8).

In order to elucidate a genetic role for *TNFAIP3* in the development of SLE and RA in the Japanese population, we investigated 2 independent case–control cohorts of patients with SLE and 3 independent cohorts of patients with RA.

PATIENTS AND METHODS

Subjects. The subjects in the SLE study group comprised 2 cohorts of Japanese patients with SLE and unrelated control subjects. An SLE case–control cohort from the RIKEN (SLE cohort 1) consisted of 376 patients (mean age 43.2 years, 90.3% women) and 934 unrelated control subjects (mean age 52.6 years, 25.0% women). An SLE case–control cohort at Hokkaido University (SLE cohort 2) consisted of 341 patients (mean age 46.2 years, 88.3% women) and 428 unrelated control subjects (mean age 47.7 years, 28.7% female). All patients with SLE fulfilled the 1997 American College of Rheumatology (ACR) revised criteria for SLE (9).

The subjects in the RA component of the study comprised 3 cohorts of Japanese patients with RA and unrelated control subjects. The first cohort of patients with RA from BioBank Japan (RA cohort 1) consisted of 1,112 patients (mean age 60.5 years, 89.7% female, 69.7% positive for rheumatoid factor [RF]), and 934 unrelated control subjects. The second cohort from RIKEN (RA cohort 2) consisted of 830 patients (mean age 64.3 years, 83.7% women, 75.0% RF positive), and 658 unrelated control subjects (mean age 48.6 years, 57.4% women). The 934 unrelated control subjects in the first cohort of RA patients were the same as those used in SLE cohort 1. An RA case–control cohort from the Institute of Rheumatology Rheumatoid Arthritis (IORRA) cohort (RA cohort 3), which is a prospective observational cohort of patients with RA studied at Tokyo Women's Medical University, comprised 1,504 patients (mean age 59.3 years, 84% women, 88% RF positive), and 752 control subjects (mean age 38.4 years, 50% women). All patients with RA met the 1987 ACR (formerly, the American Rheumatism Association) revised criteria for a diagnosis of RA (10).

All subjects entered into this study were self-identified as Japanese and were recruited through several medical institutions located in Japan. DNA samples from the patients in the first cohort of RA patients in BioBank Japan were provided by the Leading Project for Personalized Medicine from the Ministry of Education, Culture, Sports, Science and Technology, Japan (11). All subjects provided informed consent prior to their participation in this study, and the study was preapproved by the ethics committee of each institution.

SNPs. For the selection of SNPs required to genotype in and near *TNFAIP3*, we reviewed previous GWA studies of SLE and RA (3–6). We then selected 2 SNPs, rs2230926 and rs10499194. SNP rs2230926 is a nonsynonymous variant in exon 3 of *TNFAIP3* and was strongly associated with SLE in the GWA study by Musone et al (5). Although the GWA study of SLE by Graham et al indicated that rs5029939, located in intron 2 of the gene, is most significantly associated with a predisposition to SLE (6), there is strong linkage disequilibrium (LD) (r^2 = 0.86) between these SNPs according to HapMap phase II data for Japanese and evidence that rs5029939 may be substituted by rs2230926 (Figure 1). Two previous GWA studies in RA revealed that rs10499194 and rs6920220, which are located between *TNFAIP3* and *OLIG3*, were significantly associated risk variants for RA (3,4). The HapMap data for Japanese individuals indicate that the minor allele frequency (MAF) of rs6920220 is 0.011, and that the MAF for control subjects in RA cohort 3 (IORRA) was <0.01. Results of a recent study in Korean populations also indicated

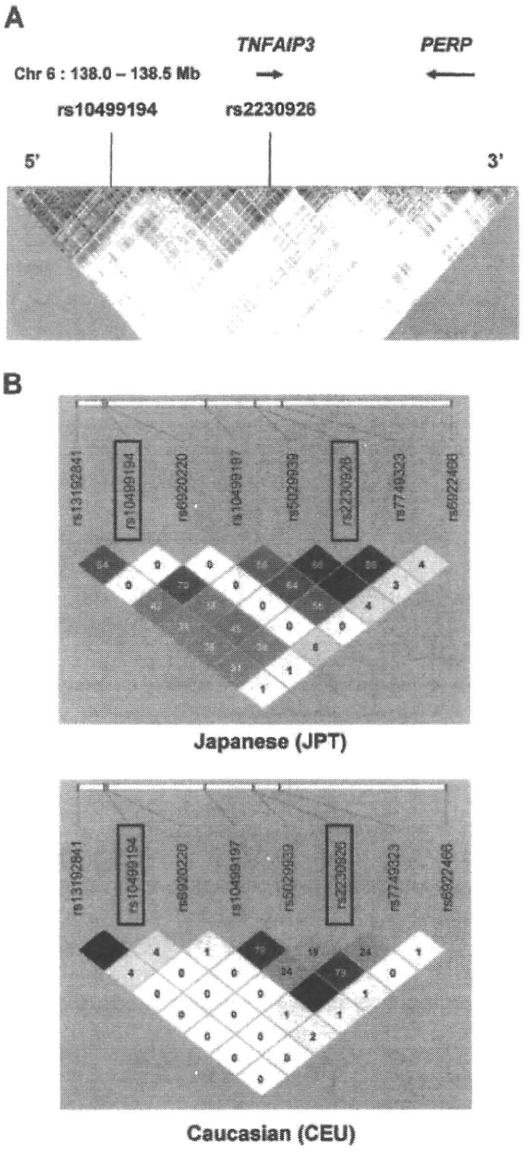

Figure 1. Pairwise linkage disequilibrium (LD) patterns for polymorphisms in the *TNFAIP3* region, according to HapMap phase II data. **A,** Pairwise LD pattern in the expanded *TNFAIP3* region derived from the HapMap data for Japanese patients, with r^2 values. *OLIG3* is located ~370 kbp away from *TNFAIP3* in the 5′ region and is not shown. **B,** Pairwise LD patterns for single-nucleotide polymorphisms (SNPs) in the *TNFAIP3* region that were significantly associated with systemic lupus erythematosus and rheumatoid arthritis in previous genome-wide association studies. The upper and lower panels were constructed using HapMap data for Japanese and Caucasian patients, respectively. The diagram shows pairwise LD values as quantified using the r^2 value. A stronger LD is depicted graphically by the densely shaded boxes. The boxed areas show the 2 SNPs genotyped.

that the variant was too rare (MAF <0.01) to be evaluated for associations (8).

Based on HapMap data for Japanese individuals, pairwise LD patterns for the SNPs in and near *TNFAIP3*, which were significantly associated with SLE and RA in the previous GWA studies, are presented in Figure 1 (for SLE, rs13192841, rs10499197, rs5029939, rs2230926, rs7749323, and rs6922466; for RA, rs10499194 and rs6920220).

Genotyping. We genotyped SNPs using TaqMan assays. For the selected SNPs, predesigned TaqMan SNP genotyping assays were used (probe ID: rs2230926, C.770116_10; rs10499194, C.1575581_10; Applied Biosystems, Foster City, CA). Fluorescence was detected using an ABI Prism 7900HT Sequence Detection System (Applied Biosystems). Genotyping assessment was performed on >98% of the samples, for all of the polymorphisms genotyped. All of the SNPs were in Hardy-Weinberg equilibrium in control subjects, according to chi-square statistics ($P > 0.01$).

Case–control association tests. We first performed allele frequency comparisons of rs2230926 and rs10499194 in SLE cohort 1 and RA cohort 1. Then, further case–control association studies were conducted using SLE cohort 2 and RA cohorts 2 and 3, to validate the associations in the first cohorts. In the replication studies, we genotyped the SNPs with a P value less than 0.05 in either SLE cohort 1 or RA cohort 1 (the P value was determined after correction for conditional logistic analysis, as described below).

Measurement of autoantibodies. Sera from 1,104 patients in RA cohort 1 were available for the measurement of anti–cyclic citrullinated peptide (anti-CCP) antibodies and RF. Anti-CCP antibodies were measured using the Mesacup CCP test (Medical and Biological Laboratories, Woburn, MA), and RF was measured by enzyme-linked immunosorbent assay.

Statistical analysis. The case–control association of each SNP was tested with the Cochran-Armitage trend test. The genotype and allele frequencies for patients and control subjects were used to calculate the odds ratios (ORs) and 95% confidence interval (95% CIs) using Woolf's method. For the combined analysis, we used the Mantel-Haenszel test. We performed conditional logistic regression analysis to evaluate the effect of each polymorphism conditional on the remaining polymorphisms, using Statistica software (StatSoft, Tulsa, OK). We calculated pairwise LD indices between pairs of SNPs (the r^2 value), using HaploView software, version 4.0 (http://www.broad.mit.edu/haploview/ haploview). We calculated the population attributable risk (PAR) using the following formula: PAR = f(OR − 1)/(1 + f[OR − 1]), where f is the allele frequency in the control subjects. PAR is defined as the reduction in incidence that would be achieved if the population had been entirely unexposed. We calculated the statistical power of association using the R software program (http://www.r-project.org).

RESULTS

Our results revealed a significant association between rs2230926 and both SLE and RA when comparing allele frequency in the patients and control subjects in the first cohort (for SLE, OR 1.92, 95% CI

Table 1. Association study of rs2230926 and rs10499194 with SLE in Japanese subjects*

dbSNP number, major/minor allele	No. of patients	No. of controls	Minor allele frequency		OR (95% CI)	*P*
			Patients	Controls		
rs2230926, G/T						
SLE 1	376	934	0.113	0.062	1.92 (1.43–2.58)	1.2×10^{-5}
SLE 2	341	428	0.116	0.064	1.91 (1.33–2.73)	3.0×10^{-4}
Combined analysis†	717	1,362	0.114	0.063	1.92 (1.53–2.41)	1.9×10^{-8}
rs10499194, T/C						
SLE 1	376	933	0.084	0.061	1.42 (1.03–1.95)	0.030

* SLE = systemic lupus erythematosus; dbSNP = Database of Single-Nucleotide Polymorphisms; OR = odds ratio; 95% CI = 95% confidence interval.
† By the Mantel-Haenszel method.

1.43–2.58, $P = 1.2 \times 10^{-5}$; for RA, OR 1.52, 95% CI 1.20–1.92, $P = 5.6 \times 10^{-4}$) (Tables 1 and 2). We also observed an association between rs10499194 and SLE patients in cohort 1 (OR 1.42, 95% CI 1.03–1.95, $P = 0.030$) (Table 1). However, the T allele appeared to represent a susceptibility allele in the SLE and RA patients in cohort 1, whereas the C allele appeared to be a risk allele for RA in Caucasians (3). We speculated that this association could be secondary to the moderate LD between rs2230926 and rs10499194 ($r^2 = 0.14$) according to data on control subjects in SLE cohort 1, and we subsequently performed a conditional logistic regression analysis to evaluate the effects of each polymorphism conditional on the remaining polymorphisms. The results of this analysis indicated that rs10499194 did not retain the statistically significant association when conditionally evaluated on rs2230926 ($P = 0.73$), while rs2230926 retained the significant association when conditionally evaluated on rs10499194 ($P = 3.4 \times 10^{-4}$). We concluded that rs2230926 was primarily associated with SLE located at this locus, and therefore genotyped only rs2230926 for replication studies in SLE (3–6).

The results of a case–control association study in SLE cohort 2 confirmed the significant association between rs2230926 and the risk of SLE (OR 1.91, 95% CI 1.33–2.73, $P = 3.0 \times 10^{-4}$). A combined analysis also confirmed a significant association (OR 1.92, 95% CI 1.53–2.41, $P = 1.9 \times 10^{-8}$, PAR = 0.055). In RA cohort 2 a statistically significant association between rs2230926 and a predisposition for RA was also replicated; however, this was not replicated in RA cohort 3 (for cohort 2, OR 1.39, 95% CI 1.07–1.81, $P = 0.013$; for cohort 3, OR 1.19, 95% CI 0.94–1.50, $P = 0.15$) (Table 2). In RA cohort 3, the statistical power required to detect an association at rs2230926 was 0.54 at a significance level of $\alpha = 0.05$ when we presumed that the OR for RA was 1.4 (the combined OR for RA cohorts 1 and 2 was 1.46). It was possible that the statistical power for RA cohort 3 may have been insufficient. A combined analysis on these data suggested a significant association (OR 1.35, 95% CI 1.18–1.56, $P = 2.6 \times 10^{-5}$, PAR = 0.024).

We observed no significant association of rs10499194 in RA cohort 1, but the statistical power to detect the association in this study was insufficient (1 –

Table 2. Association study of rs2230926 and rs10499194 with RA in Japanese subjects*

dbSNP number, minor/major allele	No. of Patients	No. of controls	Minor allele frequency		OR (95% CI)	*P*
			Patients	Controls		
rs2230926, G/T						
RA cohort 1	1,112	934	0.091	0.062	1.52 (1.20–1.92)	5.6×10^{-4}
RA cohort 2	825	655	0.100	0.074	1.39 (1.07–1.81)	0.013
RA cohort 3	1,478	747	0.087	0.075	1.19 (0.94–1.50)	0.15
Combined analysis†	3,415	2,326	0.092	0.069	1.35 (1.18–1.56)	2.6×10^{-5}
rs10499194, T/C						0.26
RA cohort 1	1,112	933	0.069	0.061	1.15 (0.90–1.48)	0.26
RA cohort 2	827	650	0.072	0.048	1.52 (1.11–2.08)	0.0090
RA cohort 3	1,472	716	0.073	0.059	1.32 (1.02–1.73)	0.038
Combined analysis†	3,411	2,299	0.071	0.056	1.30 (1.11–1.53)	8.4×10^{-4}

* RA = rheumatoid arthritis; dsSNP = Database of Single-Nucleotide Polymorphisms; OR = odds ratio; 95% CI = 95% confidence interval.
† By the Mantel-Haenszel method.

$\beta = 0.31$) considering the previously reported OR of 0.75 and a significance level of $\alpha = 0.05$ (3). Therefore, we genotyped rs10499194 in RA cohorts 2 and 3 for confirmation. Unlike in RA cohort 1, a significant association of rs10499194 was observed in RA cohorts 2 and 3 (for cohort 2, OR 1.52, 95% CI 1.11–2.08, $P = 0.0090$; for cohort 3, OR 1.32, 95% CI 1.02–1.73, $P = 0.038$) (Table 2). However, the risk allele for Caucasian patients with RA was protective against RA in our population, just as was observed in SLE cohort 1. The combined analysis showed a significant association of rs10499194 with RA (OR 1.30, 95% CI 1.11–1.53, $P = 8.4 \times 10^{-4}$).

We stratified patients in RA cohorts 1 and 3 according to the presence of anti-CCP antibodies and RF and examined for the association between *TNFAIP3* polymorphisms (rs2230926 and rs10499194) and RA susceptibility (see Supplementary Table 1, available in the online version of this article at http://www3.interscience.wiley.com/journal/76509746/home). When the patients were stratified according to anti-CCP antibody status, the G allele of rs2230926 was found to confer increased risk for RA in anti-CCP antibody–positive patients relative to anti-CCP antibody–negative patients (for anti-CCP antibody–positive patients, OR 1.36, 95% CI 1.15–1.62, $P = 4.0 \times 10^{-4}$; for anti-CCP–negative patients, OR 1.16, 95% CI 0.83–1.61, $P = 0.39$ in the combined analysis). A similar trend was observed when patients were stratified according to RF status. A stratified analysis on rs10499194 also showed that the disease susceptibility allele in Japanese patients with RA (the T allele) conferred higher risk in autoantibody-positive patients than in autoantibody-negative patients.

DISCUSSION

In the current study, rs2230926, located in exon 3 of *TNFAIP3,* was shown to be significantly associated with a predisposition to both SLE and RA in 2 and 3 independent cohorts of subjects, respectively. Our results confirmed that *TNFAIP3* is one of the common genetic risk factors for both SLE and RA, similar to *STAT4* and *IRF5*, in the Japanese and Caucasian populations (2). In addition, recent studies in Caucasian patients with RA have demonstrated that the *TNFAIP3* variant conferred an increased risk of RA in anti-CCP antibody– and RF-positive patients compared with anti-CCP antibody– and RF-negative patients (12,13). Our analysis stratified according to the autoantibodies confirmed this observation in Japanese patients with RA.

TNFAIP3 encodes a cytoplasmic zinc finger protein that is also known as the A20 protein. The A20 protein is required for negative regulation of the NF-κB signaling pathway, which is mediated by innate immune receptors such as TNF receptors and Toll-like receptors, and it prevents overstimulation of the innate immune response (7,14). The disease-associated variant, rs2230926 (T/G), is a nonsynonymous variant that results in a phenylalanine-to-cysteine change at residue 127 of the A20 protein (5). The risk allele is known to be the G allele that encodes Cys. Musone et al have reported that Cys^{127} A20 protein was only modestly, but consistently, less effective at inhibiting TNF-induced NF-κB activity than the Phe^{127} protein (5). This result suggests that reduced negative regulatory activity of A20 protein may allow excessive immune activity, leading to enhanced autoreactivity.

GWA studies of SLE patients in Caucasian populations have suggested that several polymorphisms in the *TNFAIP3* region, including the nonsynonymous SNP rs2230926, are associated with a predisposition to the disease. The genetic significance of rs2230926 was evident in the Japanese patients with SLE or RA entered into our study, although its precise role in Caucasian patients with RA remains unclear. The intergenic SNP rs10499194 is one of the landmark polymorphisms identified in Caucasian patients with RA (3,15), although the significant association with RA could not be replicated in several Caucasian populations (3,12). Because rs10499194 is also associated with RA susceptibility and autoantibody status in our population, rs10499194 could be a landmark for disease causal variants in Japanese patients with RA. However, considering the inverted susceptibility allele of rs10499194 between Japanese patients (T allele) and Caucasian patients (C allele), this association of rs10499194 would appear to be secondary, as a result of LD between rs10499194 and the disease causal variants. This finding is further supported by the lack of independent association at rs10499194 in SLE when conditioned with the rs2230926 genotype, suggesting that the association observed in rs10499194 may be partially influenced by rs2230926.

Taking into account the biologic impact of rs2230926 demonstrated by Musone et al (5), rs2230926 seems likely to be an important candidate for a causal variant in *TNFAIP3* (5). However, additional polymorphisms that are located in the intergenic region of *OLIG3* and *TNFAIP3* as well as that of *TNFAIP3* and *PERP* may also independently exercise an effect on disease susceptibility, a hypothesis that was previously raised by Musone et al (5) and Graham et al (6). Further mapping of the *TNFAIP3* region in Asian and Caucasian

populations is required for the precise determination of the additional causal polymorphisms present in patients with RA or SLE.

In conclusion, we confirm that *TNFAIP3* is a genetic risk factor for the development of both SLE and RA in the Japanese population. Although the nonsynonymous SNP rs2230926 is a strong causal variant candidate in this region, a search for additional causal variants in *TNFAIP3* is required.

ACKNOWLEDGMENTS

We are grateful to Drs. M. Yukioka, S. Tohma, Y. Nishioka, T. Matsubara, S. Wakitani, R. Teshima, and T. Sawada for their dedication in referring patients to the study and for clinical sample collection. We also thank Dr. A. Miyatake, the members of the Rotary Club of Osaka-Midosuji District 2660 Rotary International in Japan, and the staff of the BioBank Japan Project for supporting both the study and the clinical sample collection. We thank Dr. S. Tsukahara of the IORRA study and all members of the Laboratory for Autoimmune Diseases, CGM, RIKEN, for their helpful advice and excellent technical assistance.

AUTHOR CONTRIBUTIONS

All authors were involved in drafting the article or revising it critically for important intellectual content, and all authors approved the final version to be published. Dr. Kochi had full access to all of the data in the study and takes responsibility for the integrity of the data and the accuracy of the data analysis.

Study conception and design. Shimane, Kochi, Horita, Ikari, Yamada, Atsumi, Koike, Momohara, Yamanaka, Nakamura, Yamamoto.

Acquisition of data. Shimane, Kochi, Horita, Ikari, Amano, Hirakata, Okamoto, Myouzen, Suzuki, Kubo, Takasaki.

Analysis and interpretation of data. Shimane, Kochi, Horita, Ikari, Yamamoto.

REFERENCES

1. Alarcon-Segovia D, Alarcon-Riquelme ME, Cardiel MH, Caeiro F, Massardo L, Villa AR, et al. Familial aggregation of systemic lupus erythematosus, rheumatoid arthritis, and other autoimmune diseases in 1,177 lupus patients from the GLADEL cohort. Arthritis Rheum 2005;52:1138–47.
2. Gregersen PK, Olsson LM. Recent advances in the genetics of autoimmune disease. Annu Rev Immunol 2009;27:363–91.
3. Plenge RM, Cotsapas C, Davies L, Price AL, de Bakker PI, Maller J, et al. Two independent alleles at 6q23 associated with risk of rheumatoid arthritis. Nat Genet 2007;39:1477–82.
4. Thomson W, Barton A, Ke X, Eyre S, Hinks A, Bowes J, et al. Rheumatoid arthritis association at 6q23. Nat Genet 2007;39: 1431–3.
5. Musone SL, Taylor KE, Lu TT, Nititham J, Ferreira RC, Ortmann W, et al. Multiple polymorphisms in the TNFAIP3 region are independently associated with systemic lupus erythematosus. Nat Genet 2008;40:1062–4.
6. Graham RR, Cotsapas C, Davies L, Hackett R, Lessard CJ, Leon JM, et al. Genetic variants near TNFAIP3 on 6q23 are associated with systemic lupus erythematosus. Nat Genet 2008;40:1059–61.
7. Lee EG, Boone DL, Chai S, Libby SL, Chien M, Lodolce JP, et al. Failure to regulate TNF-induced NF-κB and cell death responses in A20-deficient mice. Science 2000;289:2350–4.
8. Lee HS, Korman BD, Le JM, Kastner DL, Remmers EF, Gregersen PK, et al. Genetic risk factors for rheumatoid arthritis differ in caucasian and Korean populations. Arthritis Rheum 2009;60: 364–71.
9. Hochberg MC, for the Diagnostic and Therapeutic Criteria Committee of the American College of Rheumatology. Updating the American College of Rheumatology revised criteria for the classification of systemic lupus erythematosus [letter]. Arthritis Rheum 1997;40:1725.
10. Arnett FC, Edworthy SM, Bloch DA, McShane DJ, Fries JF, Cooper NS, et al. The American Rheumatism Association 1987 revised criteria for the classification of rheumatoid arthritis. Arthritis Rheum 1988;31:315–24.
11. Nakamura Y. The BioBank Japan Project. Clin Adv Hematol Oncol 2007;5:696–7.
12. Perdigones N, Lamas JR, Vigo AG, de la Concha EG, Jover JA, Urcelay E, et al. 6q23 polymorphisms in rheumatoid arthritis Spanish patients. Rheumatology (Oxford) 2009;48:618–21.
13. Patsopoulos NA, Ioannidis JP. Susceptibility variants for rheumatoid arthritis in the TRAF1-C5 and 6q23 loci: a meta-analysis. Ann Rheum Dis 2009. E-pub ahead of print.
14. Liu YC, Penninger J, Karin M. Immunity by ubiquitylation: a reversible process of modification. Nat Rev Immunol 2005;5: 941–52.
15. Orozco G, Hinks A, Eyre S, Ke X, Gibbons LJ, Bowes J, et al. Combined effects of three independent SNPs greatly increase the risk estimate for RA at 6q23. Hum Mol Genet 2009;18:2693–9.

Arthritis Care & Research
Vol. 62, No. 5, May 2010, pp 657–663
DOI 10.1002/acr.20110

ORIGINAL ARTICLE

Change of Synovial Vascularity in a Single Finger Joint Assessed by Power Doppler Sonography Correlated With Radiographic Change in Rheumatoid Arthritis: Comparative Study of a Novel Quantitative Score With a Semiquantitative Score

JUN FUKAE,[1] YUJIRO KON,[1] MIHOKO HENMI,[1] FUMIHIKO SAKAMOTO,[1] AKIHIRO NARITA,[1] MASATO SHIMIZU,[1] KAZUHIDE TANIMURA,[1] MEGUMI MATSUHASHI,[1] TAMOTSU KAMISHIMA,[2] TATSUYA ATSUMI,[3] AND TAKAO KOIKE[3]

Objective. **To investigate the relationship between synovial vascularity assessed by quantitative power Doppler sonography (PDS) and progression of structural bone damage in a single finger joint in patients with rheumatoid arthritis (RA).**
Methods. **We studied 190 metacarpophalangeal (MCP) joints and 190 proximal interphalangeal (PIP) joints of 19 patients with active RA who had initial treatment with disease-modifying antirheumatic drugs (DMARDs). Patients were examined by clinical and laboratory assessments throughout the study. Hand and foot radiography was performed at baseline and the twentieth week. Magnetic resonance imaging (MRI) was performed at baseline. PDS was performed at baseline and the eighth week. Synovial vascularity was evaluated according to both quantitative and semiquantitative methods.**
Results. **Quantitative PDS was significantly correlated with the enhancement rate of MRI in each single finger joint. Comparing quantitative synovial vascularity and radiographic change in single MCP or PIP joints, the level of vascularity at baseline showed a significant positive correlation with radiographic progression at the twentieth week. The change of vascularity in response to DMARDs, defined as the percentage change in vascularity by the eighth week from baseline, was inversely correlated with radiographic progression in each MCP joint. The quantitative PDS method was more useful than the semiquantitative method for the evaluation of synovial vascularity in a single finger joint.**
Conclusion. **The change of synovial vascularity in a single finger joint determined by quantitative PDS could numerically predict its radiographic progression. Using vascularity as a guide to consider a therapeutic approach would have benefits for patients with active RA.**

INTRODUCTION

In recent years, the therapeutic goal for rheumatoid arthritis (RA) has moved far beyond the traditional factors of clinical remission, defined by the American College of Rheumatology (ACR) core data set or the European League Against Rheumatism (EULAR) Disease Activity Score in 28 joints (DAS28) remission criteria (1,2). To halt the progression of bone destruction, there has been a great need for a reliable predictive indicator of radiographic progression. Modern imaging techniques such as power Doppler sonography (PDS) and magnetic resonance imaging (MRI) have the potential to predict bone destruction (3–6). However, the relationship between therapeutic efficacy and image responses of these techniques has not been established.

PDS has several advantages in terms of medical cost and safety compared with other modern imaging techniques; therefore, it is more practical to use it repeatedly for monitoring disease activity. PDS detects the abnormal synovial vascular flow related to inflammation and has the potential to evaluate the level to represent this as a measurable

Clinical Trials Registration: UMIN 000002036.
[1]Jun Fukae, MD, PhD, Yujiro Kon, MD, PhD, Mihoko Henmi, MT, Fumihiko Sakamoto, MT, Akihiro Narita, MT, Masato Shimizu, MD, Kazuhide Tanimura, MD, Megumi Matsuhashi, MD: Tokeidai Memorial Hospital, Sapporo, Japan; [2]Tamotsu Kamishima, MD, PhD: Hokkaido University Hospital, Sapporo, Japan; [3]Tatsuya Atsumi, MD, PhD, Takao Koike, MD, PhD: Hokkaido University Graduate School of Medicine, Sapporo, Japan.
Address correspondence and reprint requests to Jun Fukae, MD, PhD, Center for Rheumatic Diseases, Tokeidai Memorial Hospital, Kita-1, Higashi-1, Cyuo-ku, Sapporo 060-0031, Japan. E-mail: jun.fukae@ryumachi-jp.com.
Submitted for publication October 8, 2009; accepted in revised form January 14, 2010.

Table 1. Clinical and laboratory characteristics of patients at baseline and the eighth and twentieth weeks*

	Baseline	8th week	20th week
Age, mean (range) years	54 (24–87)		
Sex, female/male	17/2		
RF positive, yes/no	15/4		
Prior use of DMARDs, yes/no	3/16		
Duration of symptoms, months	5 (3–11)		
Swollen joint count	3 (2–7)	1 (0–2)	0 (0–2)
Tender joint count	6 (2.5–13)	2 (1–5)	1 (1–1.5)
Patient's global assessment by VAS	60 (45–60)	29 (20.5–43.5)	25 (15.5–30)
ESR, mm/hour	43 (27–80)	24 (16–58)	27 (16–35)
CRP level, mg/dl	0.5 (0.25–2.82)	0.12 (0.1–1.1)	0.1 (0.1–1.4)
DAS28-ESR, mean ± SD mm/hour	5.21 ± 1.39	4.08 ± 1.60	3.56 ± 1.31

* Values are the median (interquartile range) unless otherwise indicated. RF = rheumatoid factor; DMARDs = disease-modifying antirheumatic drugs; VAS = visual analog scale; ESR = erythrocyte sedimentation rate; CRP = C-reactive protein; DAS28 = Disease Activity Score in 28 joints.

parameter (7,8). With growing interest in the ability to define remission in RA, it has been reported that abnormal synovial vascular flow still remains in individual joints after achievement of clinical remission, and therefore bone destruction would progress at a high rate in such cases (3,9). In this sense, direct assessment of synovial vascular flow in a single joint would be of use. Semiquantitative scoring has been widely used to evaluate synovial vascularity (10,11). The scoring was divided into 4 steps that were judged subjectively by the observer, and represented, accordingly, as a semiquantitative approach. The relationship between synovial vascular changes and progression of structural bone damage in a single joint has been the focus of much investigation, but only a few studies have been successful despite the intensive attempts of many researchers (3,12–14). In our preliminary study, we established quantitative PDS for synovial vascularity in each finger joint (15,16). The measurement was able to assess vascularity as quantitative data, objectively determined by the ultrasonographic program, and to detect small changes in individual finger joints. We investigated the relationship between synovial vascular changes and progression of structural bone damage in a single finger joint using the quantitative PDS measurement. We further defined the vascularity in response to disease-modifying antirheumatic drugs (DMARDs) by imaging and investigated its clinical significance in patients with active RA.

PATIENTS AND METHODS

Patients. Nineteen new patients with RA were enrolled in the study. All of the patients satisfied the ACR (formerly the American Rheumatism Association) 1987 diagnostic criteria (17). All of the patients were diagnosed as having the active state of RA according to the DAS28–erythrocyte sedimentation rate (ESR; >2.7 mm/hour). Demographic, clinical, and laboratory characteristics of the patients are shown in Table 1. Three patients were already receiving DMARDs at the initial diagnosis, but they were having no therapeutic effect (1 patient with sulfasalazine [SSZ], 2 patients with auranofin). After baseline examinations, all of the patients were given one of the new DMARDs. Initial treatments were continued throughout the study, but additional treatment and escalating doses of DMARDs were permitted in cases with disease exacerbation after the eighth week. We performed clinical and imaging examinations as mentioned in each section.

The study was conducted in accordance with the Helsinki Declaration. Informed consent to the protocol approved by the ethics committee of the hospital was obtained from all of the patients.

Ultrasonography and assessment. Ultrasonography was performed at baseline and the eighth week by 1 of the 3 ultrasonographers (MH, FS, AN) specialized in musculoskeletal ultrasonography who were blinded to other clinical information. A 13-MHz linear array transducer was used (HITACHI EUP-L34P). Pulse Doppler settings were standardized for the detection of synovial blood flow by adjusting color gain, pulse repetition, and flow optimization parameters according to a previous study (15). Power Doppler settings (75 dB dynamic range, medium persistence, medium frame rate, low wall filter, 1,300 Hz pulse repetition frequency, flow optimization: medium vein, 1,300 Hz speed velocity) were identical throughout the examinations. Room temperature was kept at 25°C. The patients were positioned comfortably, and the examinations were then started after 10 minutes of stabilization of the pulse rate. The scanning technique on each finger joint was standardized and fixed as follows: scanning of the first through fifth metacarpophalangeal (MCP) joints and the first through fifth proximal interphalangeal (PIP) joints was performed in the longitudinal plane over the dorsal surface of the joint with light skin pressure. The basic scanning technique followed the EULAR guidelines (18). The synovial vascular area with the most pronounced power Doppler activity was identified from the cine-loop and stored. The PDS images were recorded in the hard disk of the ultrasonographic machine. All of the examinations were completed within 15 minutes. Semiquantitative scoring has been described in previous studies (0 = absence of signal, 1 = single vessel dots, 2 = vessel dots over less than

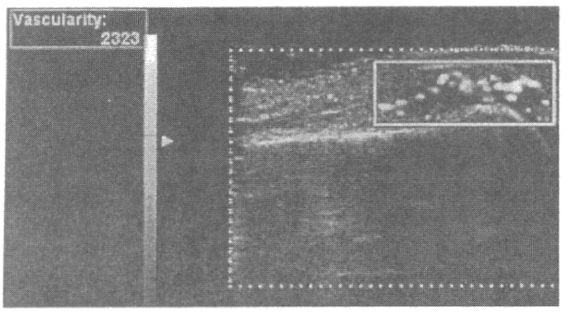

Figure 1. An image of finger joint ultrasonography (right 5th metacarpophalangeal joint). Each joint was scanned as described in the Patients and Methods section. The white line box indicates the region of interest (ROI) that was located at synovial vascular flow. Pixels of vascular flow inside the ROI were measured by the ultrasonographic program and displayed at the upper left corner of the monitor.

half of the synovium area, 3 = vessel dots over greater than half of the synovium area) (10,11,19). A synovial vascularity value, measured by quantitative PDS, was defined as P-vasc, which is the number of vascular flow pixels in the region of interest (ROI). The ROI was a standardized box type (5 mm × 10 mm) that was located to contain as many of the vascular flow pixels as possible. Vascular flow pixels in the ROI were measured automatically using the program's Vascularity mode in the ultrasonographic machine (HITACHI EUB-6500) (Figure 1).

Radiography and assessment. Plain radiographs of the hands, wrists, and feet were obtained at baseline and the twentieth week. Radiologic assessments were examined according to the Genant-modified Sharp score (GSS) by a rheumatologist (YK) who was blinded to other clinical information (20).

MRI and assessment. MRIs of both finger joints were taken at baseline using the 1.5T system (Signa Excite, version 12) with a cardiac coil. During the examination, patients were placed in the supine position with both hands on the abdomen, and these were covered by the anterior segment of the cardiac coil. Dynamic 3-dimensional forkhead activin signal transducer spoiled gradient-recalled acquisition in the steady state T1-weighted coronal images (time to recovery 500 msec, time to echo 11 msec, field of view 30 cm, matrix 256 × 160, 20 slices, slice thickness 3 mm, gap 0.4 mm, imaging time 10, 17 loops with an interval time of 5 seconds) were obtained for both hands in addition to the other images with different scan sequences. A bolus injection of gadopentate dimeglumine (Gd-DTPA; 0.1 mmole/kg body weight) was administered at 1 ml/second via a 21-gauge indwelling needle inserted into an antecubital fossa vein during acquisition of the baseline images (first loop) of the dynamic study. Data were transferred from the MRI console to a Digital Imaging and Communication in Medicine viewer and then a workstation (Advantage Windows workstation) for quantitative analysis. The severity of synovitis has been previously assessed by the rate of enhancement (E-rate) in a dynamic study by injection of Gd-DTPA (21). The E-rate indicates the index of enhancement by plotting the signal intensity against time in a selected ROI (~20–30 mm^2 in area) of the site of maximum enhancement in the above-mentioned 20 joints. Image analysis was carried out by an experienced radiologist (TK) who was blinded to other clinical information.

Statistical analysis. Statistical analyses were calculated with the use of the Excel program and the MedCalc program, version 10.4.5.0. Differences between the 2 groups were examined using either Student's *t*-test or a nonparametric test (Wilcoxon's signed rank test, Mann-Whitney U test), as applicable. A correlation between 2 variables was examined using either a parametric test (Pearson's correlation test) or a nonparametric test (Spearman's rank correlation test) according to the distribution of values. Intra-and interobserver reliability of the semiquantitative PDS score was estimated using calculations of weighted kappa statistics and overall agreement. Intra-and interobserver reliability of P-vasc was estimated using calculations of intraclass correlation coefficients (ICCs). The smallest detectable change for the radiographic score change was calculated according to a previous study (22).

RESULTS

Clinical disease activity. The mean ± SD DAS28-ESR at baseline was 5.21 ± 1.39 mm/hour. The mean ± SD DAS28-ESR at the eighth week was 4.08 ± 1.60 mm/hour, which was significantly decreased from baseline (P = 0.0001). There was no significant difference in the DAS28-ESR between the eighth week and the twentieth week (P = 0.0741). At the twentieth week, 13 patients were receiving monotherapy (9 with methotrexate [MTX], 2 with SSZ, and 2 with bucillamine) and 6 patients were receiving combination therapy of DMARDs (3 with MTX plus bucillamine, 1 with MTX plus SSZ, 1 with SSZ plus bucillamine, and 1 with SSZ plus tacrolimus). Thirteen patients were receiving oral prednisolone (3–10 mg/day) at the twentieth week.

Intra-and interobserver reliability for PDS. All PDS images for MCP joints and PIP joints were blindly evaluated twice according to the semiquantitative score for each joint by 2 ultrasonographers (MH, AN). The obtained intraobserver kappa values of the semiquantitative score were 0.944 for MCP joints and 0.930 for PIP joints. The intraobserver overall agreement for these joints was 96% and 95.4%, respectively. The obtained interobserver kappa values of the semiquantitative score were 0.950 for MCP joints and 0.923 for PIP joints. The interobserver overall agreement for these joints was 95.7% and 97.1%, respectively.

Representative images for 20 MCP joints and 20 PIP joints were randomly chosen, and P-vasc was measured 3 times each by 3 ultrasonographers (MH, FS, AN). The obtained intraobserver ICC values were 0.990 for MCP joints and 0.990 for PIP joints. The interobserver ICC values were 0.990 for MCP joints and 0.990 for PIP joints.

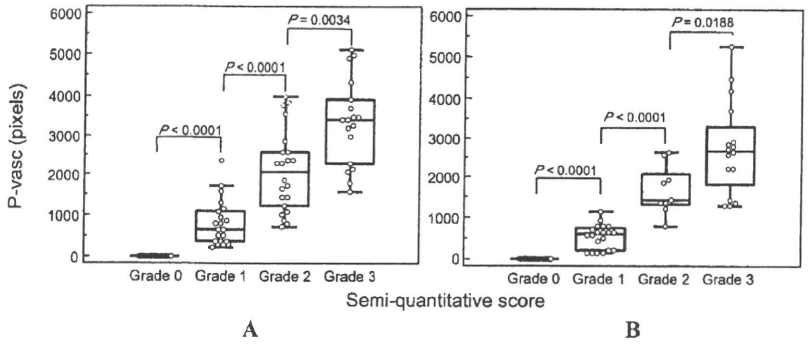

Figure 2. Relation between quantitative measurement and semi-quantitative scoring for synovial vascularity. The levels of synovial vascularity value (P-vasc) were plotted against semi-quantitative scores in MCP joints (**A**) and PIP joints (**B**).

Relationship of quantitative PDS measurement (P-vasc) to semiquantitative scoring for synovial vascularity and to the E-rate of MRI. The PDS images for 190 MCP joints and 190 PIP joints at baseline were evaluated using both the semiquantitative score and the P-vasc. The P-vasc significantly increased as the semiquantitative score increased in both MCP joints and PIP joints (Figure 2).

One patient was unable to undergo MRI because of claustrophobia. One hundred eighty MCP joints and 180 PIP joints of 18 patients were evaluated using both the P-vasc and E-rate. The P-vasc had a significant positive correlation with the E-rate of MRI in both MCP and PIP joints (Pearson's r = 0.739, $P < 0.0001$ and Pearson's r = 0.537, $P < 0.0001$, respectively) (Figure 3).

Association between vascularity and radiographic progression in a single joint. The median local GSS at baseline for MCP and PIP joints were 0 (interquartile range [IQR] 0–1) and 0.5 (IQR 0–1.5), respectively. The median local GSS at the twentieth week for MCP and PIP joints were 0.5 (IQR 0–1.5) and 0.75 (IQR 0–1.5), respectively. The median total GSS was 16.5 (IQR 11.3–37.3) at baseline. The median total GSS at the twentieth week was 30.0, which was significantly higher than the baseline score ($P = 0.001$).

We next focused on changes of single-joint P-vasc and local GSS. We investigated the association between the level of vascularity at baseline and radiographic progression at the twentieth week in each single finger joint. One hundred ninety MCP joints and 190 PIP joints at baseline were evaluated. The level of P-vasc at baseline significantly correlated with progression of the local GSS in both MCP and PIP joints (Spearman's $\rho = 0.466$, $P < 0.0001$ and Spearman's $\rho = 0.362$, $P < 0.0001$, respectively) (Figures 4A and B). The association between the semiquantitative score and the progression of the local GSS had the same tendency (data not shown). We took note of the positive PDS joints at baseline and calculated their improvement rate (IR), defined as the percentage change in P-vasc by the eighth week from baseline. The IR was calculated as follows: (P-vasc value at baseline − P-vasc value at eighth week)/P-vasc value at baseline × 100 (%). At baseline, 61 MCP joints and 44 PIP joints had positive PDS signals. The IR of P-vasc had a significant inverse correlation with local GSS progression in each single MCP joint (Spearman's $\rho = -0.340$, $P = 0.00386$) (Figure 5A). There was no significant correlation between the IR of P-vasc and local GSS progression in each single PIP joint (Spearman's $\rho = -0.223$, $P = 0.1430$) (Figure 5B). In the case of assessment by semiquantitative score, there was no significant correla-

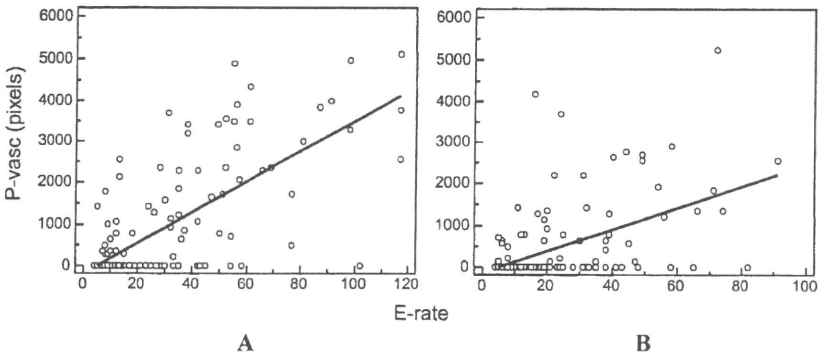

Figure 3. Relationship between quantitative measurement of synovial vascularity with power Doppler sonography and the index of synovial enhancement of magnetic resonance imaging (MRI). Scatter diagrams and regression lines of synovial vascularity value (P-vasc) against the enhancement rate (E-rate) of MRI in metacarpophalangeal joints (**A**) or proximal interphalangeal joints (**B**) are shown.

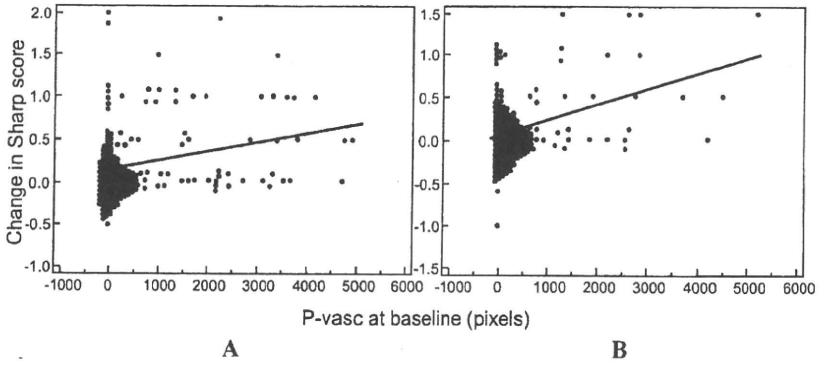

Figure 4. Relationship between the level of synovial vascularity and radiographic progression in each single finger joint. Scatter diagrams and regression lines of the synovial vascularity value (P-vasc) at baseline against progression of the local Genant-modified Sharp score from baseline to the twentieth week in metacarpophalangeal joints (**A**) or proximal interphalangeal joints (**B**) are shown.

tion to MCP or PIP joints (Spearman's $\rho = -0.256$, $P = 0.0579$ and Spearman's $\rho = -0.105$, $P = 0.5179$, respectively) (data not shown). The smallest detectable change values were calculated for the radiographic erosion score, joint space narrowing score, and combined score for single MCP and PIP joints (0.21–0.48). All of the calculated smallest detectable changes did not exceed the smallest unit of the scoring (0.5).

DISCUSSION

In this study, we quantitatively evaluated synovial vascularity in a single finger joint. In each finger joint, we found that a level of vascularity at baseline correlated with the radiographic progression. We also demonstrated that the change of vascularity in response to DMARD therapy could numerically predict the radiographic progression in each single finger joint.

We defined a standardized box type ROI and quantitatively evaluated synovial vascularity, as mentioned in the Patients and Methods section. All of the kappa values and ICCs calculated for intra-and interobserver reliability during the PDS measurements were acceptable in this study.

To demonstrate the validity of our quantitative PDS method, we first examined a relationship between the P-vasc and semiquantitative scoring. The P-vasc significantly increased in parallel with semiquantitative scoring. The E-rate of MRI is an index of Gd-DTPA enhancement indicating the inflammatory level (21,23,24), and was used for comparing with quantitative ^{99m}Tc-labeled nanocolloid scintigraphy for assessing RA (25). We next examined the relationship between the E-rate and P-vasc. Although the P-vasc was not detected in some joints with a high E-rate, a positive significant correlation was shown between the E-rate and P-vasc, suggesting that synovial vascularity determined by our quantitative PDS reflects, in part, the inflammatory level. The main reason of discrepancy between a joint with a high E-rate and negative PDS should be explained by the fact that MRI covered inflammation from all sites of synovial tissue, whereas PDS detected only from the dorsal side of synovial tissue. In addition, the difference of sensitivity of PDS and that of the E-rate might be a problem. Because the PDS is one of the advancing modalities for imaging rheumatic joints, there would be many more points to be improved in the

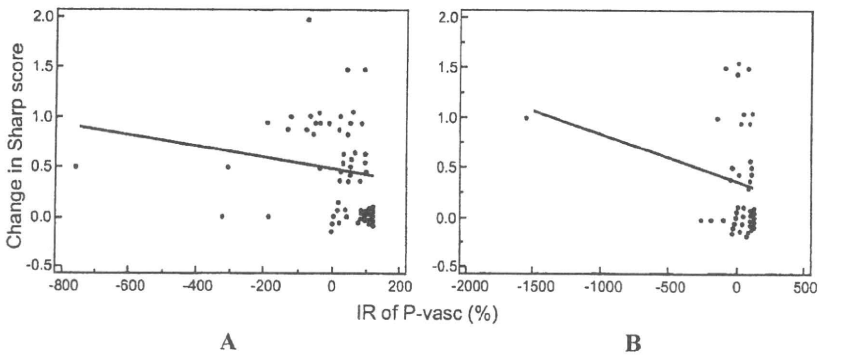

Figure 5. Relationship between improvement of synovial vascularity and radiographic progression in each single finger joint. Scatter diagrams and regression lines of the improvement rate (IR) for synovial vascularity value (P-vasc) between baseline and the eighth week against progression of the local Genant-modified Sharp score from baseline to the twentieth week in metacarpophalangeal joints (**A**) or proximal interphalangeal joints (**B**) are shown.

technological aspects, and such a process will promise to overcome the current problems in the future.

We used the P-vasc for investigating the relationship between the change of synovial vascularity and radiographic progression in a single finger joint. We found that, for each single finger joint, the baseline P-vasc significantly correlated with progression of the local GSS over 20 weeks. Our study, for the first time, has quantitatively confirmed the recent reports of Brown et al and Naredo et al that the presence of vascularity using PDS in a qualitative way correlated with the bone destruction in each single joint (3,13).

We next focused on PDS-positive finger joints at baseline and calculated each IR from baseline to the eighth week. The IR of P-vasc had a significant inverse correlation with radiographic progression in each single MCP joint. It was a novel finding that improvement in the rate of vascularity resulted in the suppression of radiographic progression. The semiquantitative score failed to demonstrate the same tendency due to its low sensitivity at detecting small changes in vascularity. On the other hand, the IR of P-vasc in PIP joints was not significantly correlated with radiographic progression, presumably due to either the sample size or the ROI setting. Further refinement of ROIs specific to PIP joints may improve the accuracy of the technique.

According to the 2002 ACR guidelines for the treatment of RA, therapeutic evaluation of first-line DMARDs was assessed at 8–12 weeks using clinical indices (26). Naredo et al reported that the time-integrated value of the PDS parameters correlated with the radiographic progression over 1 year (13), suggesting that rapid reduction in the PDS signal could predict a better radiologic prognosis. The IR of P-vasc, a change rate of 2 points, could be a useful index for preventing bone destruction. A quantitative PDS method was more useful than a semiquantitative method to detect change of synovial vascularity in each single finger joint.

Although this is a preliminary study with a small number of patients, it is noteworthy that the clinical implications of our results include the potential of synovial vascularity to numerically predict an outcome of bone destruction in each single finger joint. Furthermore, we found that the change of vascularity influenced radiographic progression. The IR of synovial vascularity should be an index of therapeutic efficacy, and therefore be of value in making judgments about additional treatment with DMARDs or to change to early biologic agent therapy. Using vascularity as guide to make therapeutic decisions at early stages would have benefits for patients with active RA. Larger and longitudinal studies would indicate the efficacy of PDS for the better management of affected patients.

ACKNOWLEDGMENT

We thank the secretary in our hospital, Ms Akemi Kitano, for data collection.

AUTHOR CONTRIBUTIONS

All authors were involved in drafting the article or revising it critically for important intellectual content, and all authors approved the final version to be submitted for publication. Dr. Fukae had full access to all of the data in the study and takes responsibility for the integrity of the data and the accuracy of the data analysis.

Study conception and design. Fukae, Kon, Tanimura, Kamishima, Atsumi, Koike.

Acquisition of data. Fukae, Kon, Henmi, Sakamoto, Narita, Shimizu, Tanimura, Matsuhashi, Kamishima.

Analysis and interpretation of data. Fukae, Kon, Henmi, Sakamoto, Narita, Shimizu, Tanimura, Matsuhashi, Kamishima, Atsumi, Koike.

REFERENCES

1. Felson DT, Anderson JJ, Boers M, Bombardier C, Furst D, Goldsmith C, et al. American College of Rheumatology preliminary definition of improvement in rheumatoid arthritis. Arthritis Rheum 1995;38:727–35.
2. Prevoo ML, van 't Hof MA, Kuper HH, van Leeuwen MA, van de Putte LB, van Riel PL. Modified disease activity scores that include twenty-eight–joint counts: development and validation in a prospective longitudinal study of patients with rheumatoid arthritis. Arthritis Rheum 1995;38:44–8.
3. Brown AK, Conaghan PG, Karim Z, Quinn MA, Ikeda K, Peterfy CG, et al. An explanation for the apparent dissociation between clinical remission and continued structural deterioration in rheumatoid arthritis. Arthritis Rheum 2008;58:2958–67.
4. Freeston JE, Brown AK, Hensor EM, Emery P, Conaghan PG. Extremity magnetic resonance imaging assessment of synovitis (without contrast) in rheumatoid arthritis may be less accurate than power Doppler ultrasound [letter]. Ann Rheum Dis 2008;67:1351.
5. Freeston JE, Bird P, Conaghan PG. The role of MRI in rheumatoid arthritis: research and clinical issues. Curr Opin Rheumatol 2009;21:95–101.
6. Haavardsholm EA, Ostergaard M, Hammer HB, Boyesen P, Boonen A, van der Heijde D, et al. Monitoring anti-TNFα treatment in rheumatoid arthritis: responsiveness of magnetic resonance imaging and ultrasonography of the dominant wrist compared to conventional measures of disease activity and structural damage. Ann Rheum Dis 2009;68:1572–9.
7. Naredo E, Bonilla G, Gamero F, Uson J, Carmona L, Laffon A. Assessment of inflammatory activity in rheumatoid arthritis: a comparative study of clinical evaluation with grey scale and power Doppler ultrasonography. Ann Rheum Dis 2005;64:375–81.
8. Szkudlarek M, Narvestad E, Klarlund M, Court-Payen M, Thomsen HS, Ostergaard M. Ultrasonography of the metatarsophalangeal joints in rheumatoid arthritis: comparison with magnetic resonance imaging, conventional radiography, and clinical examination. Arthritis Rheum 2004;50:2103–12.
9. Brown AK, Quinn MA, Karim Z, Conaghan PG, Peterfy CG, Hensor E, et al. Presence of significant synovitis in rheumatoid arthritis patients with disease-modifying antirheumatic drug–induced clinical remission: evidence from an imaging study may explain structural progression. Arthritis Rheum 2006;54:3761–73.
10. Newman JS, Laing TJ, McCarthy CJ, Adler RS. Power Doppler sonography of synovitis: assessment of therapeutic response. Preliminary observations. Radiology 1996;198:582–4.
11. Hau M, Schultz H, Tony HP, Keberle M, Jahns R, Haerten R, et al. Evaluation of pannus and vascularization of the metacarpophalangeal and proximal interphalangeal joints in rheumatoid arthritis by high-resolution ultrasound (multidimensional linear array). Arthritis Rheum 1999;42:2303–8.
12. Taylor PC, Steuer A, Gruber J, Cosgrove DO, Blomley MJ, Marsters PA, et al. Comparison of ultrasonographic assessment of synovitis and joint vascularity with radiographic